Networks and Heterogeneous Media

https://www.aimspress.com/journal/nhm

NHM, 21(4): 1393–1425.
DOI: 10.3934/nhm.2026053
Received: 02 May 2026
Revised: 23 June 2026
Accepted: 23 June 2026
Published: 03 July 2026

Research article

Sheffer-type lacunary bivariate q-Laguerre polynomials with applications to heterogeneous graph filters

Waseem Ahmad Khan[1], **Oğuz Yağcı**[2], **Khidir Shaib Mohamed**[3,*], **Azhar Iqbal**[4,5], **Wei Sin Koh**[6] **and Naglaa Mohammed**[3]

[1] Department of Electrical Engineering, Prince Mohammad Bin Fahd University, P.O. Box 1664, Al Khobar 31952, Saudi Arabia

[2] Department of Mathematics, Kırıkkale University, Kırıkkale 71450, Türkiye

[3] Department of Mathematics, College of Science, Qassim University, Buraidah 51452, Saudi Arabia

[4] Department of Mathematics and Natural Sciences, Prince Mohammad Bin Fahd University, P.O. Box 1664, Al Khobar 31952, Saudi Arabia

[5] Cognitive Intelligence and AI Systems, Prince Mohammad Bin Fahd University, P.O. Box 1664, Al Khobar 31952, Saudi Arabia

[6] Faculty of Business and Communications, INTI International University, Nilai 71800, Negeri Sembilan, Malaysia

* **Correspondence:** Email: k.idris@qu.edu.sa.

Abstract: We introduce a lacunary bivariate q-Laguerre–Sheffer family generated by the product of a Sheffer factor, a first q-exponential, and a q-Tricomi–Bessel kernel. The construction has three independent controls: the lacunarity index fixes which powers enter the finite sums, the kernel order changes the Bessel-type shifts, and the Sheffer factor supplies an additional deformation of the sequence. We derive explicit coefficient and convolution formulas, lowering relations, a quasi-monomial operator structure, a q-difference equation, and a q-translation identity. We then evaluate the polynomials at a mass-weighted graph Laplacian associated with heterogeneous network diffusion. This gives polynomial spectral filters whose vertex-domain support is limited to a prescribed graph-hop radius. Numerical examples illustrate the locality bound, spectral response tuning, comparison with a Chebyshev polynomial filter, kernel truncation accuracy, and a one-parameter calibration problem.

Keywords: q-Laguerre polynomials; m-lacunary polynomials; Sheffer sequences; quasi-monomiality; q-Tricomi–Bessel functions; numerical methods; process innovation; graph Laplacians; heterogeneous networks; spectral graph filters
Mathematics Subject Classification: 33D45, 39A13, 05A30, 05C50, 65M70

1. Introduction

Quantum calculus (q-calculus), originating in Jackson's theory of q-difference equations and developed in the modern notation of basic hypergeometric series, replaces ordinary differentiation by q-difference operators and provides a natural framework for basic hypergeometric functions, discrete models, and deformation problems; see [1–4]. Within this setting, generating functions and operational methods are particularly useful because they produce identities compatible with the deformation limit $q \to 1^-$, where the corresponding continuous formulas are recovered.

The classical theory of q-Laguerre polynomials is built on several complementary viewpoints. Moak [5] developed a systematic q-analogue of the Laguerre polynomials, Askey [6] clarified limiting relations among q-Laguerre families, and Cigler [7] showed how operator methods generate q-identities for Laguerre-type systems. These foundational papers are important for the present work because they establish the three ingredients that are used below: q-factorial coefficient scales, deformation limits, and operator realizations. They also explain why q-Laguerre families are a suitable testing ground for combining generating functions, q-difference equations, and quasi-monomiality.

A second line of work concerns bivariate and Appell-type extensions of q-Laguerre polynomials. Cao et al., [8] constructed two-variable q-Laguerre polynomials from the viewpoint of quasi-monomiality, while Bao and Yang [9] emphasized q-partial differential equations for homogeneous q-Laguerre and little q-Jacobi families. Ahmad and Khan [10] treated a generalized q-Laguerre-based Appell class with quasi-monomiality; Qawaqneh et al., [11] developed structural properties and applications for generalized bivariate q-Laguerre polynomials; Zayed et al., [12] investigated extended bivariate q-Laguerre-based Appell polynomials; and Kumar et al., [13] considered q-Mittag-Leffler–Laguerre polynomials. Together, these contributions show that the Appell and bivariate settings preserve much of the Laguerre structure while allowing additional deformation parameters and applications.

The Sheffer and general-Appell viewpoints provide the broader algebraic mechanism behind these constructions, going back to Appell's original polynomial sequences and the classical theory of Sheffer sequences and finite operator/umbral calculus [14–17]. Khan and Raza [18] used the monomiality principle and operational methods to study Laguerre–Sheffer polynomials, Özat et al. [19] studied Laguerre-type general-Appell polynomials, Khan et al. [20] considered mth-order Laguerre-based Appell polynomials, and Mohammed et al., [21] used q-operational methods for q-Legendre-based Gould–Hopper polynomials. These works are relevant here because the arbitrary invertible factor $A_q(t)$ in our generating function is precisely the Sheffer-type component that converts a core Laguerre system into a flexible umbral family.

The kernel side is governed by Tricomi–Bessel-type functions. Dattoli et al., [22] studied generating functions for Bessel and Laguerre–Tricomi functions; Riyasat et al., [23] developed q-Tricomi functions in connection with quantum algebra representations; Nahid and Rani [24] treated Mittag-Leffler-based Bessel and Tricomi functions through an umbral approach; Fadel et al., [25] obtained representations for q-Bessel functions; and Zainab and Kumar [26] studied integral identities involving λ-Bessel and λ-Tricomi matrix functions. The importance of these works for the present construction is that the kernel order λ is not merely a parameter in a generating function; it controls the shift relations produced by q-differentiation in the x-variable. Lacunary generating functions form another relevant background, and the Laguerre case studied by Babusci et al., [27] motivates the use of the substitution $t \mapsto t^m$ to isolate residue classes.

The applied motivation comes from spectral models on weighted networks and heterogeneous media. For a weighted graph G, the graph Laplacian and its normalized or mass-weighted variants are basic operators in spectral graph theory and graph signal processing [28, 29]. They also arise as finite-dimensional spatial operators in diffusion and evolution equations on networks [30]. If a diagonal mass matrix M represents heterogeneous storage, density, or nodal capacity, then the semi-discrete diffusion equation

$$M\dot{u}(t) + L_G u(t) = 0$$

is transformed by $v = M^{1/2}u$ into $\dot{v}(t) + Hv(t) = 0$, where $H = M^{-1/2}L_G M^{-1/2}$ is self-adjoint and positive semidefinite. Polynomial functions of H therefore provide localized spectral filters and finite-hop surrogate operators. The lacunary bound $\lfloor n/m \rfloor$ in the family introduced below is particularly useful in this setting because, for each fixed polynomial index n, it reduces the graph-hop radius from the full degree n to at most $\lfloor n/m \rfloor$.

Recent advances in computational mathematics also motivate the cost-aware presentation adopted here. High-order multi-step iterations for nonlinear systems, kernel/RBF neural-network solvers for diffusion-type PDEs, compact finite-difference formulas generated from RBFs with polynomial augmentation, and RBF–FD schemes for partial integro-differential models show that analytic structure is most useful in practice when it is paired with explicit operation counts and stable implementable formulas [31–34]. Related application-oriented models, such as Rayleigh-tail/GARCH risk quantification, similarly illustrate the value of formulas that retain interpretability while remaining numerically tractable [35]. In this broader landscape, the present construction is positioned not only as a symbolic extension of q-Laguerre–Sheffer theory but also as a finite-sum framework with graph-locality bounds, truncation diagnostics, and parameter-calibration mechanisms.

This paper combines two structural features that are usually treated separately in the bivariate q-Laguerre literature: (i) a genuine m-lacunary mechanism implemented by the substitution $t \mapsto t^m$, and (ii) a Sheffer-type deformation obtained by allowing an arbitrary invertible prefactor $A_q(t)$. For $m \in \mathbb{N}$, $\lambda \in \mathbb{N}_0$, and an invertible q-exponential generating series $A_q(t) = \sum_{j=0}^{\infty} a_j t^j/[\, j\,]_q!$ with $a_0 \neq 0$, we define the (m, λ)-lacunary bivariate q-Laguerre–Sheffer family $\{\mathcal{L}_{n,q}^{(m,\lambda;A)}(x, y)\}_{n\geq 0}$ by the following normalized generating identity:

$$\begin{aligned} &A_q(t)\, e_q(yt)\, C_{\lambda,q}(-xt^m) \\ &\quad = \left(\sum_{j=0}^{\infty} a_j \frac{t^j}{[\, j\,]_q!}\right)\left(\sum_{r=0}^{\infty} y^r \frac{t^r}{[\, r\,]_q!}\right)\left(\sum_{k=0}^{\infty} \frac{x^k t^{mk}}{[\, k\,]_q!\,[\, \lambda + k\,]_q!}\right) = \sum_{n=0}^{\infty} \mathcal{L}_{n,q}^{(m,\lambda;A)}(x, y)\, \frac{t^n}{[\, n\,]_q!}. \end{aligned} \tag{1.1}$$

Here, e_q is the first q-exponential in the standard q-calculus notation [2, 3], and

$$C_{\lambda,q}(x) = \sum_{k=0}^{\infty} \frac{(-1)^k x^k}{[\, k\,]_q!\,[\, \lambda + k\,]_q!}$$

is the λ-order q-Tricomi–Bessel kernel, in line with the Tricomi–Bessel and q-Tricomi conventions used in [22, 23]. The expanded middle expression in Eq 1.1 fixes the sign and normalization: substituting $-xt^m$ into $C_{\lambda,q}$ changes $(-1)^k(-x)^k$ into x^k. The lacunary substitution implies that the coefficient of t^n depends only on $k \leq \lfloor n/m \rfloor$, and hence the core sequence decomposes naturally according to the residue class of n mod m.

Let us emphasize the precise point at which the present construction differs from earlier bivariate q-Laguerre, q-Laguerre–Appell, and lacunary generating-function models. If one suppresses any one of the three ingredients, m, λ, and A_q, then one recovers known families listed in Section 4. Here these ingredients are retained simultaneously: m fixes a residue-class lacunarity, λ shifts the order of the q-Tricomi–Bessel kernel, and the arbitrary invertible factor A_q produces a full Sheffer deformation rather than only a translation or Appell-type perturbation. This simultaneous treatment produces operator identities in which the x-lowering changes the kernel order while the y-lowering preserves it; this mixed behavior is absent from the non-lacunary and fixed-order special cases.

The main contributions are the following. First, we give a finite coefficient formula and an explicit residue-class/degree profile showing exactly how the lacunary part is embedded in the Sheffer convolution. Second, we derive two compatible lowering mechanisms, one in y and one in x, including the mixed q-partial differential relation. Third, we formulate the quasi-monomial structure in the formal q-operator algebra, with a careful treatment of inverses and q-commutators. Fourth, we convert the formal family into a concrete network tool by evaluating it at a heterogeneous graph Laplacian $H = M^{-1/2}L_G M^{-1/2}$ and proving the corresponding finite-hop locality property. Fifth, the computational section is expanded beyond zero plots by including a graph-filter example, truncation diagnostics for the kernel, and a one-parameter recovery problem for the Sheffer twist.

From Eq 1.1 we derive (a) a finite coefficient representation; (b) a q-binomial Sheffer convolution formula; and (c) a quasi-monomial description with explicit raising/lowering operators, the associated operator q-difference equation, and a q-translation formula. We also record parameter-shift relations for $C_{\lambda,q}$, discuss the limit $q \to 1^-$, summarize specializations that recover several earlier bivariate q-Laguerre-type families, and show how the same formulas act as localized graph filters on heterogeneous networks.

The paper is organized as follows. Section 2 reviews the required q-calculus notation and the λ-order q-Tricomi–Bessel kernel. Section 3 develops coefficient formulas, convolution identities, and the operational/quasi-monomial framework. Section 4 collects specializations and links with earlier bivariate q-Laguerre-type constructions. Section 5 discusses the classical limit $q \to 1^-$. Section 6 presents a heterogeneous graph-filter application, computational illustrations, and a simple parameter-calibration example. Section 7 concludes the paper.

2. Preliminaries

Throughout the formal identities are understood for $0 < |q| < 1$ whenever the displayed q-factorials are nonzero. In the analytic, limiting, positivity, and numerical parts, and in particular in all discussions of the limit $q \to 1^-$, we specialize to $0 < q < 1$. We use the standard q-numbers and q-factorials of q-calculus and basic hypergeometric series [2–4]

$$[\,\alpha\,]_q = \frac{1-q^\alpha}{1-q}, \qquad [\,n\,]_q! = \prod_{k=1}^{n}[\,k\,]_q, \qquad [\,0\,]_q! = 1, \tag{2.1}$$

and the q-binomial coefficients

$$\begin{bmatrix} n \\ k \end{bmatrix}_q = \frac{[\,n\,]_q!}{[\,k\,]_q!\,[\,n-k\,]_q!}, \qquad 0 \le k \le n. \tag{2.2}$$

For $a \in \mathbb{C}$ and $n \in \mathbb{N}_0$ we write (see [3,4])

$$(a;q)_0 = 1, \qquad (a;q)_n = \prod_{j=0}^{n-1}(1-aq^j), \qquad (a;q)_\infty = \prod_{j=0}^{\infty}(1-aq^j),$$

so that $(q;q)_n = (1-q)^n\,[\,n\,]_q!$. We shall use the following normalized q-Bessel-type series notation:

$${}_0\phi_1(-;b;q,z) := \sum_{k=0}^{\infty} \frac{z^k}{(b;q)_k\,(q;q)_k}.$$

This convention is stated explicitly to avoid confusion with the Gasper–Rahman basic hypergeometric normalization, in which additional powers of q occur in the general definition of ${}_r\phi_s$ [3,4].

The first q-exponential, with the normalization used in Jackson-type q-calculus [1–3], is

$$e_q(z) = \sum_{n=0}^{\infty} \frac{z^n}{[\,n\,]_q!}. \tag{2.3}$$

For a variable $z \neq 0$, we use the Jackson q-derivative [1,2]

$$D_{q,z}f(z) = \frac{f(qz)-f(z)}{(q-1)z}, \tag{2.4}$$

extended continuously at $z = 0$. In particular, $D_{q,y} := D_{q,y}$ and $D_{q,x}$ satisfy $D_{q,z}z^n = [\,n\,]_q\,z^{n-1}$ for $n \geq 1$, hence

$$D_{q,y}\,y^n = [\,n\,]_q\,y^{n-1}, \qquad n \geq 1. \tag{2.5}$$

The q-addition polynomial associated with the product rule for first q-exponentials is denoted by $\oplus_q$ and defined by [2,3]

$$(y \oplus_q z)^n := \sum_{r=0}^{n} \begin{bmatrix} n \\ r \end{bmatrix}_q y^{n-r}z^r, \qquad n \in \mathbb{N}_0. \tag{2.6}$$

Equivalently, coefficient comparison gives

$$e_q((y \oplus_q z)t) = e_q(yt)e_q(zt). \tag{2.7}$$

Lemma 2.1. *For every complex number α, one has*

$$D_{q,y}\,e_q(\alpha y) = \alpha\,e_q(\alpha y). \tag{2.8}$$

Proof. Differentiate Eq 2.3 termwise and use Eq 2.5:

$$D_{q,y}e_q(\alpha y) = \sum_{n\geq 1} \frac{\alpha^n}{[\,n\,]_q!}[\,n\,]_q\,y^{n-1} = \alpha \sum_{n\geq 0} \frac{(\alpha y)^n}{[\,n\,]_q!} = \alpha e_q(\alpha y).$$

We work with the following λ-order q-Tricomi–Bessel kernel, a q-analogue of the Laguerre–Tricomi/Bessel kernel used in umbral and operational treatments of special functions [22, 23]:

$$C_{\lambda,q}(x) = \sum_{k=0}^{\infty} \frac{(-1)^k x^k}{[\,k\,]_q!\,[\,\lambda+k\,]_q!}, \qquad \lambda \in \mathbb{N}_0. \tag{2.9}$$

Proposition 2.2. *For $\lambda \in \mathbb{N}_0$, one has*

$$C_{\lambda,q}(x) = \frac{(1-q)^\lambda}{(q;q)_\lambda}\, {}_0\phi_1\Big(-;q^{\lambda+1};q,-(1-q)^2x\Big). \tag{2.10}$$

Proof. Using $[\,k\,]_q! = (q;q)_k/(1-q)^k$ and $(q;q)_{\lambda+k} = (q;q)_\lambda(q^{\lambda+1};q)_k$, we rewrite Eq 2.9 as

$$C_{\lambda,q}(x) = \frac{(1-q)^\lambda}{(q;q)_\lambda} \sum_{k=0}^{\infty} \frac{(-(1-q)^2x)^k}{(q^{\lambda+1};q)_k\,(q;q)_k},$$

which is exactly Eq 2.10.

Lemma 2.3. *For $\lambda \in \mathbb{N}_0$, one has the parameter-shift identity*

$$D_{q,x}C_{\lambda,q}(x) = -\,C_{\lambda+1,q}(x). \tag{2.11}$$

Proof. Differentiate Eq 2.9 termwise and use $D_{q,x}x^k = [\,k\,]_q x^{k-1}$:

$$D_{q,x}C_{\lambda,q}(x) = \sum_{k\geq 1} \frac{(-1)^k[\,k\,]_q x^{k-1}}{[\,k\,]_q!\,[\,\lambda+k\,]_q!} = \sum_{k\geq 1} \frac{(-1)^k x^{k-1}}{[\,k-1\,]_q!\,[\,\lambda+k\,]_q!}.$$

With the change of index $j = k-1$, this becomes

$$-\sum_{j\geq 0} \frac{(-1)^j x^j}{[\,j\,]_q!\,[\,\lambda+1+j\,]_q!} = -C_{\lambda+1,q}(x).$$

Setting $\lambda = 0$ in Eq 2.9 gives $[\,\lambda+k\,]_q! = [\,k\,]_q!$ for every $k \geq 0$. Therefore, the denominator becomes the square of the same q-factorial, and the kernel reduces to

$$C_{0,q}(x) = \sum_{k=0}^{\infty} \frac{(-1)^k x^k}{([\,k\,]_q!)^2}. \tag{2.12}$$

This is the order-zero q-Tricomi–Bessel kernel used in the standard two-variable q-Laguerre specialization; see, for example, [8, 10].

3. The (m,λ)-lacunary q-Laguerre–Sheffer family

In this section, we develop the structural consequences of the generating function in Eq 3.2 using the standard generating-function and Sheffer-sequence viewpoint of finite operator calculus [15–18]. Unless a statement is explicitly identified as a specialization of an earlier family, the definitions, lemmas, propositions, corollaries, and theorems in this section are new in the simultaneous $(m,\lambda;A)$ form considered here. Their derivations combine coefficient extraction, lacunary residue separation, and formal Sheffer inversion; these methods are rooted in the cited umbral and q-Laguerre literature, but the present combination of the lacunarity index m, the kernel order λ, and the arbitrary invertible factor A_q does not appear in those references.

3.1. Definition and generating function

Definition 3.1. Fix $m \in \mathbb{N}$ and $\lambda \in \mathbb{N}_0$, and let

$$A_q(t) = \sum_{j=0}^{\infty} a_j \frac{t^j}{[\,j\,]_q!}, \qquad a_0 \neq 0, \tag{3.1}$$

be an invertible formal power series in the usual Sheffer/umbral sense [15, 17]. We define the sequence $\{\mathcal{L}_{n,q}^{(m,\lambda;A)}(x,y)\}_{n\geq 0}$ via the generating function

$$A_q(t)\, e_q(yt)\, C_{\lambda,q}(-xt^m) = \sum_{n=0}^{\infty} \mathcal{L}_{n,q}^{(m,\lambda;A)}(x,y)\, \frac{t^n}{[\,n\,]_q!}. \tag{3.2}$$

The core family $\mathcal{L}_{n,q}^{(m,\lambda)}(x,y)$ corresponds to $A_q(t) \equiv 1$.

Remark 3.2. The factor t^m makes the family m-lacunary in x, as in lacunary generating-function theory for Laguerre-type polynomials [27], which leads to $n \leftrightarrow n-m$ recurrences. The series $A_q(t)$ provides a Sheffer-type deformation in the sense of the classical Sheffer and umbral frameworks [15–17].

3.2. Coefficient formula, residue profile, and Sheffer convolution

The next coefficient formula extends the standard generating-function extraction used for two-variable q-Laguerre and q-Laguerre–Appell polynomials and incorporates the residue-class mechanism familiar from lacunary Laguerre generating functions [8, 10, 27].

Theorem 3.3. *For each $n \in \mathbb{N}_0$, the polynomial $\mathcal{L}_{n,q}^{(m,\lambda;A)}(x,y)$ has the explicit form*

$$\mathcal{L}_{n,q}^{(m,\lambda;A)}(x,y) = [\,n\,]_q! \sum_{k=0}^{\lfloor n/m \rfloor} \sum_{j=0}^{n-mk} \frac{a_j\, x^k\, y^{n-mk-j}}{[\,j\,]_q!\,[\,n-mk-j\,]_q!\,[\,k\,]_q!\,[\,\lambda+k\,]_q!}. \tag{3.3}$$

Proof. Expand $A_q(t)$, $e_q(yt)$, and $C_{\lambda,q}(-xt^m)$ in Eq 3.2. Since

$$C_{\lambda,q}(-xt^m) = \sum_{k\geq 0} \frac{x^k t^{mk}}{[\,k\,]_q!\,[\,\lambda+k\,]_q!},$$

the coefficient of t^n in the product is

$$\sum_{k=0}^{\lfloor n/m \rfloor} \sum_{j=0}^{n-mk} \frac{a_j\, x^k\, y^{n-mk-j}}{[\,j\,]_q!\,[\,n-mk-j\,]_q!\,[\,k\,]_q!\,[\,\lambda+k\,]_q!}.$$

By Eq 3.2, this coefficient equals $\mathcal{L}_{n,q}^{(m,\lambda;A)}(x,y)/[\,n\,]_q!$, so multiplying by $[\,n\,]_q!$ gives Eq 3.3.

Remark 3.4.
For fixed n, put $K = \lfloor n/m \rfloor$. The finite double sum in Eq 3.3 contains

$$N_{n,m} = \sum_{k=0}^{K} (n-mk+1) = (K+1)(n+1) - \frac{mK(K+1)}{2} \tag{3.4}$$

scalar summands. If the coefficients a_j, the q-factorials, and the required powers of x and y are precomputed recursively, a direct evaluation therefore requires $O(N_{n,m})$ arithmetic operations and $O(n+K)$ stored scalar data, or only $O(1)$ extra memory if the powers and factorial ratios are updated on the fly. For fixed m, this is $O(n^2/m)$, whereas the core case Eq 3.5 has only $K+1 = \lfloor n/m \rfloor + 1$ summands. Thus, the Sheffer prefactor A_q adds flexibility at the cost of changing the single lacunary sum into a triangular finite convolution.

Corollary 3.5. *If $A_q(t) \equiv 1$ (i.e. $a_0 = 1$ and $a_j = 0$ for $j \geq 1$), then*

$$\mathcal{L}_{n,q}^{(m,\lambda)}(x,y) = [\,n\,]_q! \sum_{k=0}^{\lfloor n/m \rfloor} \frac{x^k\, y^{n-mk}}{[\,n-mk\,]_q!\,[\,k\,]_q!\,[\,\lambda+k\,]_q!}. \tag{3.5}$$

Proof. Set $j = 0$ in Eq 3.3.

The following residue profile is the precise form taken here by the lacunary decomposition of Laguerre-type generating functions; compare the lacunary Laguerre framework in [27] and the two-variable q-Laguerre setting in [8].

Proposition 3.6. *Let $n = m\ell + s$ with $0 \leq s < m$. The core polynomial satisfies*

$$\mathcal{L}_{m\ell+s,q}^{(m,\lambda)}(x,y) = [\,m\ell+s\,]_q! \sum_{k=0}^{\ell} \frac{x^k y^{m(\ell-k)+s}}{[\,m(\ell-k)+s\,]_q!\,[\,k\,]_q!\,[\,\lambda+k\,]_q!}. \tag{3.6}$$

Consequently, only powers of y congruent to s modulo m occur in the core family. For a general Sheffer prefactor A_q, the same residue-filtered core components are combined through

$$\mathcal{L}_{n,q}^{(m,\lambda;A)}(x,y) = \sum_{j=0}^{n} \begin{bmatrix} n \\ j \end{bmatrix}_q a_j\, \mathcal{L}_{n-j,q}^{(m,\lambda)}(x,y), \tag{3.7}$$

so A_q mixes the residue classes in a controlled q-Sheffer convolution.

Proof. Equation 3.6 is Eq 3.5 written with $n = m\ell + s$. Since $n - mk = m(\ell - k) + s$, each exponent of y is congruent to s modulo m. The formula in Eq 3.7 follows by multiplying the core generating function by $A_q(t)$ and extracting the coefficient of t^n; the same coefficient comparison is recorded as the Sheffer convolution identity in Theorem 3.7 below.

Theorem 3.7. *The Sheffer-type family satisfies the convolution identity*

$$\mathcal{L}_{n,q}^{(m,\lambda;A)}(x,y) = \sum_{j=0}^{n} \begin{bmatrix} n \\ j \end{bmatrix}_q a_j\, \mathcal{L}_{n-j,q}^{(m,\lambda)}(x,y). \tag{3.8}$$

Proof. Rewrite Eq 3.2 as

$$A_q(t) \sum_{r\geq 0} \mathcal{L}_{r,q}^{(m,\lambda)}(x,y) \frac{t^r}{[\,r\,]_q!} = \sum_{n\geq 0} \mathcal{L}_{n,q}^{(m,\lambda;A)}(x,y) \frac{t^n}{[\,n\,]_q!}.$$

Extracting the coefficient of t^n yields

$$\frac{\mathcal{L}_{n,q}^{(m,\lambda;A)}(x,y)}{[\,n\,]_q!} = \sum_{j=0}^{n} a_j\, \frac{\mathcal{L}_{n-j,q}^{(m,\lambda)}(x,y)}{[\,j\,]_q!\,[\,n-j\,]_q!},$$

which is equivalent to Eq 3.8.

3.3. Lowering operators and mixed q-partial relations

Theorem 3.8. *For $n \geq 1$, one has*

$$D_{q,y}\,\mathcal{L}_{n,q}^{(m,\lambda;A)}(x,y) = [\,n\,]_q\,\mathcal{L}_{n-1,q}^{(m,\lambda;A)}(x,y). \tag{3.9}$$

Proof. Apply $D_{q,y}$ to Eq 3.2. By Lemma 2.1, $D_{q,y}e_q(yt) = t\,e_q(yt)$. Hence

$$\sum_{n\geq 0}\left(D_{q,y}\mathcal{L}_{n,q}^{(m,\lambda;A)}(x,y)\right)\frac{t^n}{[\,n\,]_q!} = t\sum_{n\geq 0}\mathcal{L}_{n,q}^{(m,\lambda;A)}(x,y)\frac{t^n}{[\,n\,]_q!} = \sum_{n\geq 1}\mathcal{L}_{n-1,q}^{(m,\lambda;A)}(x,y)\frac{t^n}{[\,n-1\,]_q!}.$$

Comparing the coefficients of t^n for $n \geq 1$ gives Eq 3.9.

The m-lacunary structure implies that x-differentiation naturally lowers the degree by m and shifts the kernel order. This yields a second lowering relation, now in the x-variable.

Lemma 3.9. *For $\lambda \in \mathbb{N}_0$ and $m \in \mathbb{N}$, one has*

$$D_{q,x}\,C_{\lambda,q}(-xt^m) = t^m\,C_{\lambda+1,q}(-xt^m). \tag{3.10}$$

Proof. Expand $C_{\lambda,q}(-xt^m) = \sum_{k\geq 0} x^k t^{mk}/([\,k\,]_q![\,\lambda+k\,]_q!)$ and apply $D_{q,x}$ termwise:

$$D_{q,x}C_{\lambda,q}(-xt^m) = \sum_{k\geq 1}\frac{[\,k\,]_q x^{k-1}t^{mk}}{[\,k\,]_q![\,\lambda+k\,]_q!} = \sum_{k\geq 1}\frac{x^{k-1}t^{mk}}{[\,k-1\,]_q![\,\lambda+k\,]_q!}.$$

Changing the index to $j = k-1$ gives $t^m\sum_{j\geq 0} x^j t^{mj}/([\,j\,]_q![\,\lambda+1+j\,]_q!)$, which is Eq 3.10.

Theorem 3.10. *For $n \geq m$, one has*

$$D_{q,x}\,\mathcal{L}_{n,q}^{(m,\lambda;A)}(x,y) = \Big(\prod_{r=0}^{m-1}[\,n-r\,]_q\Big)\,\mathcal{L}_{n-m,q}^{(m,\lambda+1;A)}(x,y), \tag{3.11}$$

whereas $D_{q,x}\,\mathcal{L}_{n,q}^{(m,\lambda;A)}(x,y) = 0$ for $0 \leq n < m$.

Proof. Apply $D_{q,x}$ to Eq 3.2 and use Lemma 3.9:

$$\sum_{n\geq 0}\left(D_{q,x}\mathcal{L}_{n,q}^{(m,\lambda;A)}(x,y)\right)\frac{t^n}{[\,n\,]_q!} = t^m A_q(t)e_q(yt)C_{\lambda+1,q}(-xt^m).$$

The right-hand side equals $t^m\sum_{n\geq 0}\mathcal{L}_{n,q}^{(m,\lambda+1;A)}(x,y)\,t^n/[\,n\,]_q!$. Hence

$$\frac{D_{q,x}\mathcal{L}_{n,q}^{(m,\lambda;A)}(x,y)}{[\,n\,]_q!} = \frac{\mathcal{L}_{n-m,q}^{(m,\lambda+1;A)}(x,y)}{[\,n-m\,]_q!} \qquad (n \geq m),$$

which is equivalent to Eq 3.11. For $n < m$ there is no matching term, so the derivative vanishes.

Corollary 3.11. *For $n \geq m$,*

$$D_{q,x}\,\mathcal{L}_{n,q}^{(m,\lambda;A)}(x,y) = D_{q,y}^m\,\mathcal{L}_{n,q}^{(m,\lambda+1;A)}(x,y), \tag{3.12}$$

where $D_{q,y}$ acts with respect to y. Such mixed q-partial differential relations are in the spirit of the q-PDE approach to homogeneous q-Laguerre families (see, e.g., [9]).

Proof. Apply Theorem 3.8 m times to $\mathcal{L}_{n,q}^{(m,\lambda+1;A)}$ and compare with Eq 3.11.

3.4. Operational representation and quasi-monomiality

The following operational representation follows the monomiality-principle approach to Laguerre-type and q-special polynomial systems [7, 18, 19].

Theorem 3.12. *Let $A_q(D_{q,y}) = \sum_{j\geq 0} a_j D_{q,y}^j/[\,j\,]_q!$. Then, for every $n \geq 0$,*

$$\mathcal{L}_{n,q}^{(m,\lambda;A)}(x,y) = A_q(D_{q,y})\, C_{\lambda,q}(-xD_{q,y}^m)\,\{y^n\}. \tag{3.13}$$

Proof. Interpret $A_q(D_{q,y})$ and $C_{\lambda,q}(-xD_{q,y}^m)$ as formal series in $D_{q,y}$. Acting on y^n and using $D_{q,y}^r\{y^n\} = [\,n\,]_q!\, y^{n-r}/[\,n-r\,]_q!$ for $r \leq n$ produces exactly the double sum in Eq 3.3, so Eq 3.13 follows.

Remark 3.13.

The formula in Eq 3.3 is usually the most transparent option for scalar evaluation at low or moderate degrees and for reproducibility checks: the summation limits are explicit, the lacunary depth is visible, and the implementation reduces to precomputed q-factorials and powers. Its main numerical drawbacks are the quadratic term count in the full Sheffer case and the possible cancellation among signed or complex coefficients when A_q oscillates or when x and y have competing scales. The operational form in Eq 3.13, by contrast, is better suited to structured computation: it can exploit recurrence, lowering relations, sparse graph powers, or matrix-vector products when x is replaced by an operator, such as a graph Laplacian. Its disadvantage is that one must choose a polynomial basis or truncation strategy for the formal operators, so it is not automatically cheaper for a single scalar value. In practice, Eq 3.3 is preferable for direct tabulation and validation, while Eq 3.13 is preferable when repeated evaluations, operator arguments, or sparse linear-algebra structure can be reused.

Define

$$\Phi(D_{q,y}) := A_q(D_{q,y})\, C_{\lambda,q}(-xD_{q,y}^m). \tag{3.14}$$

Then, Eq 3.13 reads $\mathcal{L}_n = \Phi(D_{q,y})\{y^n\}$. Since $A_q(0) = a_0 \neq 0$ and $C_{\lambda,q}(0) = 1/[\,\lambda\,]_q! \neq 0$, the formal series $\Phi(D_{q,y})$ has non-zero constant term and is therefore invertible in the ring of formal power series in $D_{q,y}$, as customary in umbral calculus [16, 17]. All quotients, such as $\Phi(qD_{q,y})/\Phi(D_{q,y})$, below are understood in this formal sense. Similarly,

$$\Delta_q F(D_{q,y}) = \frac{F(D_{q,y}) - F(qD_{q,y})}{(1-q)D_{q,y}}$$

should not be read as an analytic division by the lowering operator $D_{q,y}$. The numerator has zero constant term, so there is a unique formal series $G(D_{q,y})$ satisfying $F(D_{q,y}) - F(qD_{q,y}) = (1-q)D_{q,y}\, G(D_{q,y})$; this series is denoted by $\Delta_q F(D_{q,y})$.

Lemma 3.14. *For every $r \in \mathbb{N}$,*

$$D_{q,y}^r\, y = q^r\, y\, D_{q,y}^r + [\,r\,]_q\, D_{q,y}^{r-1}. \tag{3.15}$$

Proof. For any test polynomial $f(y)$, the q-product rule gives

$$D_{q,y}(yf)(y) = \frac{qyf(qy) - yf(y)}{(q-1)y} = f(y) + qyD_{q,y}f(y).$$

Thus, the operator identity is $D_{q,y}\, y = 1 + q\, y\, D_{q,y}$, where the symbol y denotes multiplication by y and the constant term 1 denotes the identity operator. This convention avoids treating $D_{q,y}y$ as an ordinary scalar product. Assume that Eq 3.15 holds for some $r \geq 1$. Multiplying the identity by $D_{q,y}$ on the left and again using $D_{q,y}\, y = 1 + q\, y\, D_{q,y}$, we obtain

$$D^{r+1}_{q,y} y = q^r (D_{q,y} y) D^r_{q,y} + [\, r\,]_q D^r_{q,y} = q^{r+1} y D^{r+1}_{q,y} + (q^r + [\, r\,]_q) D^r_{q,y}.$$

Since $q^r + [\, r\,]_q = [\, r+1\,]_q$, this is Eq 3.15 with r replaced by $r+1$.

Lemma 3.15. *Let $F(D_{q,y}) = \sum_{r\geq 0} c_r D^r_{q,y}$ be a formal series. Then,*

$$F(D_{q,y})\, y = y\, F(qD_{q,y}) + \Delta_q F(D_{q,y}), \tag{3.16}$$

where

$$\Delta_q F(D_{q,y}) := \frac{F(D_{q,y}) - F(qD_{q,y})}{(1-q) D_{q,y}}. \tag{3.17}$$

Proof. By linearity it suffices to take $F(D_{q,y}) = D^r_{q,y}$. Lemma 3.14 gives

$$D^r_{q,y} y = q^r y D^r_{q,y} + [\, r\,]_q D^{r-1}_{q,y} = y(qD_{q,y})^r + \Delta_q (D^r_{q,y}),$$

because $\Delta_q(D^r_{q,y}) = [\, r\,]_q D^{r-1}_{q,y}$. Summing over r yields Eq 3.16.

The next raising and lowering operators express the quasi-monomial structure in the usual operational sense [18, 19, 22].

Theorem 3.16. *Define*

$$\widehat{P} := D_{q,y}, \qquad \widehat{M} := \Phi(D_{q,y})\, y\, \Phi(D_{q,y})^{-1}. \tag{3.18}$$

Then, for all $n \geq 0$,

$$\widehat{P}\, \mathcal{L}^{(m,\lambda;A)}_{n,q}(x,y) = [\, n\,]_q\, \mathcal{L}^{(m,\lambda;A)}_{n-1,q}(x,y), \qquad \widehat{M}\, \mathcal{L}^{(m,\lambda;A)}_{n,q}(x,y) = \mathcal{L}^{(m,\lambda;A)}_{n+1,q}(x,y). \tag{3.19}$$

Proof. Since $\Phi(D_{q,y})$ is a series in $D_{q,y}$, it commutes with $D_{q,y}$. Using $\mathcal{L}_n = \Phi(D_{q,y})\{y^n\}$ we get

$$\widehat{P}\, \mathcal{L}_n = D_{q,y}\, \Phi(D_{q,y})\{y^n\} = \Phi(D_{q,y})\{D_{q,y} y^n\} = [\, n\,]_q\, \Phi(D_{q,y})\{y^{n-1}\} = [\, n\,]_q\, \mathcal{L}_{n-1}.$$

Moreover,

$$\widehat{M}\, \mathcal{L}_n = \Phi(D_{q,y})\, y\, \Phi(D_{q,y})^{-1}\, \Phi(D_{q,y})\{y^n\} = \Phi(D_{q,y})\{y^{n+1}\} = \mathcal{L}_{n+1}.$$

Theorem 3.17. *With Φ from Eq 3.14, the raising operator admits the decomposition*

$$\widehat{M} = y\, \frac{\Phi(qD_{q,y})}{\Phi(D_{q,y})} + \frac{\Delta_q \Phi(D_{q,y})}{\Phi(D_{q,y})}. \tag{3.20}$$

Here, both quotients are products with the formal inverse of $\Phi(D_{q,y})$, whose existence follows from $\Phi(0) \neq 0$.

Proof. Lemma 3.15 applied to $F(D_{q,y}) = \Phi(D_{q,y})$ gives

$$\Phi(D_{q,y})\, y = y\,\Phi(qD_{q,y}) + \Delta_q\Phi(D_{q,y}).$$

Multiplying on the right by $\Phi(D_{q,y})^{-1}$ gives

$$\Phi(D_{q,y})y\Phi(D_{q,y})^{-1} = y\,\Phi(qD_{q,y})\Phi(D_{q,y})^{-1} + \Delta_q\Phi(D_{q,y})\Phi(D_{q,y})^{-1},$$

which is exactly Eq 3.20.

It is convenient to interpret the pair $(\widehat{P}, \widehat{M})$ in Theorem 3.16 as a representation of a q-deformed Heisenberg–Weyl algebra. For two operators, X and Y, we use the standard q-commutator notation [2,7].

$$[X, Y]_q := XY - q\,YX.$$

The basic q-product rule implies the elementary relation

$$[D_{q,y}, y]_q = 1, \qquad \text{i.e.,} \qquad D_{q,y}\, y - q\, y\, D_{q,y} = 1. \tag{3.21}$$

Proposition 3.18. *With* $\widehat{P} = D_{q,y}$ *and* $\widehat{M} = \Phi(D_{q,y})\, y\, \Phi(D_{q,y})^{-1}$*, we have*

$$[\widehat{P}, \widehat{M}]_q = 1. \tag{3.22}$$

Proof. Since $\Phi(D_{q,y})$ is a series in $D_{q,y}$, it commutes with $D_{q,y}$. Hence,

$$\begin{aligned}\widehat{P}\widehat{M} - q\,\widehat{M}\widehat{P} &= D_{q,y}\,\Phi(D_{q,y})y\Phi(D_{q,y})^{-1} - q\,\Phi(D_{q,y})y\Phi(D_{q,y})^{-1}D_{q,y}\\ &= \Phi(D_{q,y})(D_{q,y}\,y - q\,y\,D_{q,y})\Phi(D_{q,y})^{-1}.\end{aligned}$$

Using Eq 3.21 gives Eq 3.22.

Corollary 3.19. *For every* $n \in \mathbb{N}$*,*

$$\widehat{P}\,\widehat{M}^{\,n} = [\,n\,]_q\,\widehat{M}^{\,n-1} + q^n\,\widehat{M}^{\,n}\widehat{P}. \tag{3.23}$$

Proof. The case $n = 1$ is Eq 3.22. Assume that Eq 3.23 holds for n. Then,

$$\widehat{P}\widehat{M}^{n+1} = (\widehat{P}\widehat{M}^{n})\widehat{M} = ([\,n\,]_q\widehat{M}^{n-1} + q^n\widehat{M}^n\widehat{P})\widehat{M} = [\,n\,]_q\widehat{M}^n + q^n\widehat{M}^n(\widehat{P}\widehat{M}).$$

Using $\widehat{P}\widehat{M} = 1 + q\,\widehat{M}\widehat{P}$ from Eq 3.22 yields

$$\widehat{P}\widehat{M}^{n+1} = ([\,n\,]_q + q^n)\widehat{M}^n + q^{n+1}\widehat{M}^{n+1}\widehat{P} = [\,n+1\,]_q\widehat{M}^n + q^{n+1}\widehat{M}^{n+1}\widehat{P},$$

which is Eq 3.23 with n replaced by $n + 1$.

Remark 3.20. The q-commutation relation in Eq 3.22 and the eigen-operator identity in Proposition 3.21 are standard signatures of quasi-monomial sequences and operational methods in q-calculus; see, for example, [2, 7].

Proposition 3.21. *For all* $n \geq 0$*,*

$$\widehat{M}\,\widehat{P}\,\mathcal{L}_{n,q}^{(m,\lambda;A)}(x, y) = [\,n\,]_q\,\mathcal{L}_{n,q}^{(m,\lambda;A)}(x, y). \tag{3.24}$$

Proof. By Theorem 3.16, $\widehat{P}\mathcal{L}_n = [\,n\,]_q\mathcal{L}_{n-1}$. Applying $\widehat{M}$ gives $\widehat{M}\widehat{P}\mathcal{L}_n = [\,n\,]_q\mathcal{L}_n$.

Proposition 3.22. *Let* $R(D_{q,y}) = \Phi(qD_{q,y})/\Phi(D_{q,y})$ *and* $S(D_{q,y}) = \Delta_q\Phi(D_{q,y})/\Phi(D_{q,y})$*. Then,*

$$\Big(yR(D_{q,y})D_{q,y} + S(D_{q,y})D_{q,y} - [\,n\,]_q\Big)\,\mathcal{L}_{n,q}^{(m,\lambda;A)}(x, y) = 0. \tag{3.25}$$

Proof. Substitute Eq 3.20 into Eq 3.24 and use $\widehat{P} = D_{q,y}$.

3.5. q-translation

We now use the q-addition operation defined in Eq 2.6.

Theorem 3.23. *For all $n \geq 0$,*

$$\mathcal{L}^{(m,\lambda;A)}_{n,q}(x, y \oplus_q z) = \sum_{r=0}^{n} \begin{bmatrix} n \\ r \end{bmatrix}_q \mathcal{L}^{(m,\lambda;A)}_{n-r,q}(x, y)\, z^r. \tag{3.26}$$

Proof. Replace y by $y \oplus_q z$ in Eq 3.2. By Eq 2.7, $e_q((y \oplus_q z)t) = e_q(yt)\, e_q(zt)$. The generating function then factors as

$$\sum_{n\geq 0} \mathcal{L}_n(x, y \oplus_q z)\frac{t^n}{[\,n\,]_q!} = \left(\sum_{n\geq 0} \mathcal{L}_n(x, y)\frac{t^n}{[\,n\,]_q!}\right)\left(\sum_{r\geq 0} \frac{z^r t^r}{[\,r\,]_q!}\right),$$

so extracting the coefficient of t^n gives Eq 3.26.

4. Special cases and links with existing families

This section records parameter choices in Eq 3.2 that recover several bivariate q-Laguerre-type families from the recent literature on q-Laguerre–Appell polynomials and quasi-monomiality [8, 10, 12]. The statements below are included as either cited recoveries of known families or new specialization identities of the present generating function. We abbreviate $\mathcal{L}^{(m,\lambda;A)}_{n,q}(x, y) := \mathcal{L}^{(m,\lambda;A)}_{n,q}(x, y)$.

4.1. Comparison with prior work and novelty

Table 1 should be read together with the following distinction. Earlier bivariate q-Laguerre constructions emphasize the two-variable q-Laguerre core and its quasi-monomial structure, while q-Laguerre–Appell models add a general Appell or Sheffer prefactor without simultaneously retaining a separate lacunary index and a variable Tricomi–Bessel order. Lacunary Laguerre generating functions, on the other hand, isolate residue classes through substitutions, such as $t \mapsto t^m$, but they do not by themselves include the present q-Sheffer deformation. The present family keeps all three mechanisms in the same generating function: m controls residue-class lacunarity and graph-hop degree, λ controls the order shift of the q-Tricomi–Bessel kernel, and $A_q(t)$ gives an arbitrary invertible Sheffer factor.

Table 1. Parameter choices in Eq 3.2 leading to selected families.

Parameters	Resulting family	Reference
$A_q(t) \equiv 1$, $\lambda = 0$, general m	mth-order bivariate q-Laguerre	[8]
$A_q(t) \equiv 1$, $\lambda = 0$, $m = 2$	bivariate q-Laguerre	[8]
general $A_q(t)$, $\lambda = 0$, $m = 2$	bivariate q-Laguerre–Appell	[10, 11]
general $A_q(t)$, $\lambda = 0$, general m	mth-order Laguerre-based Appell-type	[12, 20]
general $A_q(t)$, general λ, general m	Sheffer-type (m, λ)-lacunary family	present work

From the graph-filter point of view, the construction is also different from standard Chebyshev or heat-kernel polynomial filters. Those filters usually begin with a desired scalar multiplier and then approximate it by a polynomial basis. Here, the polynomial basis is inherited from the q-Laguerre–Sheffer generating function, so the same formula provides both symbolic lowering/raising identities and a finite-hop graph multiplier. The comparison in Section 6.2 is included to place this response beside a standard Chebyshev polynomial benchmark.

4.2. Recovering earlier families

Corollary 4.1. *Assume $A_q(t) \equiv 1$ and $\lambda = 0$. Then, Eq 3.2 reduces to*

$$e_q(yt)\, C_{0,q}(-xt^m) = \sum_{n=0}^{\infty} \mathcal{L}_{n,q}^{(m,0)}(x,y)\, \frac{t^n}{[\,n\,]_q!},$$

which matches the mth-order two-variable q-Laguerre polynomials in [8]. Moreover,

$$\mathcal{L}_{n,q}^{(m,0)}(x,y) = [\,n\,]_q! \sum_{k=0}^{\lfloor n/m \rfloor} \frac{x^k\, y^{n-mk}}{[\,n-mk\,]_q!\,([\,k\,]_q!)^2}. \tag{4.1}$$

Proof. This is the core case of Definition 3.1. Equation 4.1 is Corollary 3.5 with $\lambda = 0$.

Corollary 4.2. *If $m = 2$ and $A_q(t) \equiv 1$, then $\mathcal{L}_{n,q}^{(2,\lambda)}(x,y)$ is the bivariate q-Laguerre family with generating function*

$$e_q(yt)\, C_{\lambda,q}(-xt^2) = \sum_{n=0}^{\infty} \mathcal{L}_{n,q}^{(2,\lambda)}(x,y)\, \frac{t^n}{[\,n\,]_q!}.$$

For $\lambda = 0$ this specializes to the bivariate q-Laguerre polynomials studied in [8].

Corollary 4.3. *If $m = 2$ and $\lambda = 0$, then Eq 3.2 becomes*

$$A_q(t)\, e_q(yt)\, C_{0,q}(-xt^2) = \sum_{n=0}^{\infty} \mathcal{L}_{n,q}^{(2,0;A)}(x,y)\, \frac{t^n}{[\,n\,]_q!},$$

which gives a q-Laguerre–Appell deformation comparable to the constructions in [10, 11].

Corollary 4.4. *If $\lambda = 0$ and the q-exponential factor is replaced by $e_q(yt^m)$, then one obtains the extended Laguerre-based Appell setting considered, for example, in [12]. The same approach applies with minor changes.*

A particularly transparent specialization is obtained by choosing

$$A_q(t) = e_q(\alpha t) = \sum_{j=0}^{\infty} \alpha^j \frac{t^j}{[\,j\,]_q!}, \qquad \alpha \in \mathbb{C}.$$

This choice corresponds to a q-translation in the y-variable. The first few members of this shifted family are listed in Table 2.

Proposition 4.5. *Let $\mathcal{L}_{n,q}^{(m,\lambda;\alpha)}(x,y)$ be defined by Eq 3.2 with $A_q(t) = e_q(\alpha t)$. Then,*

$$\mathcal{L}_{n,q}^{(m,\lambda;\alpha)}(x,y) = \mathcal{L}_{n,q}^{(m,\lambda)}(x,\, y \oplus_q \alpha). \tag{4.2}$$

Equivalently,

$$\mathcal{L}_{n,q}^{(m,\lambda;\alpha)}(x,y) = \sum_{r=0}^{n} \begin{bmatrix} n \\ r \end{bmatrix}_q \mathcal{L}_{n-r,q}^{(m,\lambda)}(x,y)\, \alpha^r. \tag{4.3}$$

Proof. Since $e_q((y \oplus_q \alpha)t) = e_q(yt)e_q(\alpha t)$, the generating function in Eq 3.2 with $A_q(t) = e_q(\alpha t)$ becomes

$$e_q((y \oplus_q \alpha)t)\, C_{\lambda,q}(-xt^m) = \sum_{n\geq 0} \mathcal{L}^{(m,\lambda;\alpha)}_{n,q}(x,y)\frac{t^n}{[\,n\,]_q!},$$

which is precisely the core generating function with y replaced by $y \oplus_q \alpha$. This gives Eq 4.2. The expansion in Eq 4.3 is then a direct application of the q-translation formula Eq 3.26 with $z = \alpha$.

Table 2. First members of the q-shifted family $\mathcal{L}^{(2,0;\alpha)}_{n,q}(x,y)$.

n	$\mathcal{L}^{(2,0;\alpha)}_{n,q}(x,y)$
0	1
1	$y \oplus_q \alpha$
2	$(y \oplus_q \alpha)^2 + [\,2\,]_q!\, x$
3	$(y \oplus_q \alpha)^3 + [\,3\,]_q!\, x\,(y \oplus_q \alpha)$
4	$(y \oplus_q \alpha)^4 + \dfrac{[\,4\,]_q!}{[\,2\,]_q!}\, x\,(y \oplus_q \alpha)^2 + \dfrac{[\,4\,]_q!}{([\,2\,]_q!)^2}\, x^2$

5. The classical limit $q \to 1^-$

The q-lacunary Sheffer family reduces, in the limit $q \to 1^-$, to a classical lacunary Laguerre–Sheffer structure generated by the Tricomi–Bessel kernel. The limiting statements below combine the standard q-factorial and q-exponential limits [2,3] with the classical Bessel-Tricomi series representation [22,36]; the resulting lacunary Sheffer limit is new for the simultaneous $(m,\lambda;A)$ family.

Proposition 5.1. *For each fixed $\lambda \in \mathbb{N}_0$ and $x \in \mathbb{C}$,*

$$\lim_{q\to 1^-} C_{\lambda,q}(x) = C_\lambda(x) := \sum_{k=0}^{\infty} \frac{(-1)^k x^k}{k!\,(\lambda+k)!}.$$

Moreover, $C_\lambda(x) = x^{-\lambda/2} J_\lambda(2\sqrt{x})$, where J_λ is the Bessel function of the first kind; this follows directly from the standard power-series representation of J_λ [22, 24, 36].

Proof. It is standard that $[\,n\,]_q! \to n!$ and hence $e_q(z) \to e^z$ as $q \to 1^-$ [2]. Applying these termwise in Eq 2.9 yields the stated series. The Bessel connection follows by matching with the series for J_λ.

Theorem 5.2. *Assume $A_q(t) \to A(t)$ coefficientwise as $q \to 1^-$. Then, the generating function in Eq 3.2 converges to*

$$A(t)\, e^{yt}\, C_\lambda(-xt^m) = \sum_{n=0}^{\infty} \mathcal{L}^{(m,\lambda;A)}_n(x,y)\,\frac{t^n}{n!}, \tag{5.1}$$

which defines a classical Sheffer-type (m,λ)-lacunary bivariate Laguerre family. In particular, the x-lowering relation in Eq 3.11 tends to

$$\partial_x\, \mathcal{L}^{(m,\lambda;A)}_n(x,y) = n(n-1)\cdots(n-m+1)\, \mathcal{L}^{(m,\lambda+1;A)}_{n-m}(x,y).$$

Remark 5.3. When $A(t) \equiv 1$ the limit family is governed purely by the lacunary mechanism and the Tricomi-Bessel kernel, which connects to the lacunary generating-function literature for Laguerre polynomials (see, e.g., [27] and references therein).

6. Application to heterogeneous graph filters and numerical illustrations

This section connects the coefficient representation in Eq 3.3 with a concrete network calculation and then gives computational illustrations of the core and Sheffer-deformed families. The graph notation and spectral-filter interpretation follow standard conventions from spectral graph theory and graph signal processing [28, 29, 37, 38]. The finite-hop locality result is a new consequence of applying the present lacunary q-Laguerre–Sheffer polynomial to a sparse graph operator, while the walk-support argument is the standard one for powers of graph Laplacian-type matrices [28, 29]. The purpose is not merely to display zeros, but to record reproducible diagnostics: graph-hop locality, degree profiles, root statistics, truncation errors, and a parameter-recovery experiment. All plots and numerical values were generated by direct evaluation of Eq 3.3 with $0 < q < 1$.

6.1. *A finite-hop filter for a heterogeneous weighted network*

Let $G = (V, E, w)$ be an undirected weighted graph with N vertices and weighted Laplacian L_G, in the standard spectral graph theory notation [28]. Let

$$M = \mathrm{diag}(m_1, \ldots, m_N), \qquad m_i > 0,$$

be a diagonal matrix of heterogeneous nodal masses, storage coefficients, or capacities; such weighted network diffusion formulations are commonly treated through semigroup and network-evolution methods [30]. The network diffusion equation

$$M\dot{u}(t) + L_G u(t) = 0 \tag{6.1}$$

is equivalent, under the change of variable $v = M^{1/2}u$, to

$$\dot{v}(t) + Hv(t) = 0, \qquad H = M^{-1/2} L_G M^{-1/2}.$$

Thus, H is the natural self-adjoint graph operator for a heterogeneous network.

This discrete model may be viewed as a finite-dimensional analogue of heterogeneous diffusion in continuum media. For example, a variable-coefficient diffusion equation with spatially varying storage or density leads, after finite-volume, finite-element, or network discretization, to a mass matrix and a stiffness/Laplacian matrix. In finite-element terminology, M is the lumped mass matrix and L_G plays the role of the stiffness matrix, while in finite-volume terminology the edge weights represent discrete flux conductances between control volumes. The diagonal matrix M used here represents the simplest lumped-mass version of that mechanism. Hence, the graph setting is not a full continuum heterogeneous-media model, but a network discretization in which heterogeneity enters through both nodal masses and edge conductivities.

For scalar parameters $\tau > 0$ and $\eta \in \mathbb{C}$ we define the (m, λ)-lacunary q-Laguerre–Sheffer graph filter, following the usual practice of defining graph filters as polynomial or spectral functions of a graph Laplacian [29, 37, 38],

$$\mathcal{F}_{n,q}^{(m,\lambda;A)}(H; \tau, \eta) := \mathcal{L}_{n,q}^{(m,\lambda;A)}(\tau H, \eta I_N). \tag{6.2}$$

Using Eq 3.3, this is the finite matrix polynomial

$$\mathcal{F}_{n,q}^{(m,\lambda;A)}(H;\tau,\eta) = [\,n\,]_q! \sum_{k=0}^{\lfloor n/m \rfloor} \sum_{j=0}^{n-mk} \frac{a_j\,\tau^k \eta^{n-mk-j}}{[\,j\,]_q!\,[\,n-mk-j\,]_q!\,[\,k\,]_q!\,[\,\lambda+k\,]_q!}\, H^k. \tag{6.3}$$

In Eqs 6.2 and 6.3, the substitution $x = \tau H$ and $y = \eta I_N$ is evaluated in the commutative polynomial sense: H commutes with I_N, so the scalar monomials $x^k y^r$ in Eq 3.3 become $\tau^k \eta^r H^k$ without any ordering ambiguity.

Consequently, the filter degree in the graph operator is at most $\lfloor n/m \rfloor$, not n in general. The parameter m controls this graph-hop bound, λ changes the Tricomi-Bessel spectral weighting, and A_q supplies a tunable Sheffer response. Equivalently, if ξ is a spectral variable for H, then the scalar response of the filter is the polynomial

$$p_{n,q}^{(m,\lambda;A)}(\xi;\tau,\eta) := [\,n\,]_q! \sum_{k=0}^{\lfloor n/m \rfloor} \sum_{j=0}^{n-mk} \frac{a_j\,\tau^k \eta^{n-mk-j}}{[\,j\,]_q!\,[\,n-mk-j\,]_q!\,[\,k\,]_q!\,[\,\lambda+k\,]_q!}\, \xi^k. \tag{6.4}$$

Thus, the same finite coefficient formula simultaneously gives a localized vertex-domain operator and a scalar spectral transfer function.

Proposition 6.1. *If the sparsity pattern of H is that of G together with diagonal entries, then*

$$\left(\mathcal{F}_{n,q}^{(m,\lambda;A)}(H;\tau,\eta)\right)_{rs} = 0 \qquad \textit{whenever} \qquad \mathrm{dist}_G(r,s) > \lfloor n/m \rfloor.$$

Thus, the lacunary index m gives a finite-hop locality bound for the graph filter.

Proof. For any matrix H whose off-diagonal nonzero pattern is supported on the edges of G, the entry $(H^k)_{rs}$ can be nonzero only if there exists a walk of length at most k from r to s; diagonal entries only allow waiting steps and do not reduce graph distance. The formula in Eq 6.3 involves powers H^k only for $0 \le k \le \lfloor n/m \rfloor$, so all entries at larger graph distance vanish.

We illustrate this construction on the five-node path graph with edge conductivities

$$w_{12} = 1.0, \qquad w_{23} = 0.6, \qquad w_{34} = 1.4, \qquad w_{45} = 0.8,$$

and heterogeneous masses

$$(m_1, m_2, m_3, m_4, m_5) = (1.00, 2.00, 0.75, 1.50, 1.25).$$

The graph, edge weights, masses, and injected unit impulse are shown in Figure 1. For $(m,\lambda,q,n,\tau,\eta) = (2,0,0.6,8,0.20,1)$ and $A_q(t) \equiv 1$, the degree in H is $\lfloor 8/2 \rfloor = 4$. In this case

$$\mathcal{F}_{8,0.6}^{(2,0)}(H;0.20,1) = I + 1.1946005312H + 0.5128452574H^2 + 0.1138725796H^3 + 0.0076957572H^4. \tag{6.5}$$

The finite coefficient profile in Figure 2 makes the hop truncation explicit: no power H^k with $k > 4$ is present.

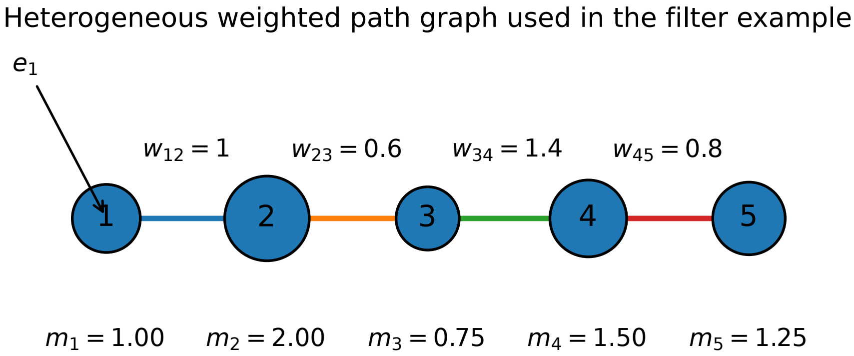

Figure 1. Heterogeneous weighted path graph used in the finite-hop filter example. Node sizes are proportional to the masses m_i, edge labels show the conductivities w_{ij}, and the arrow indicates the unit impulse e_1.

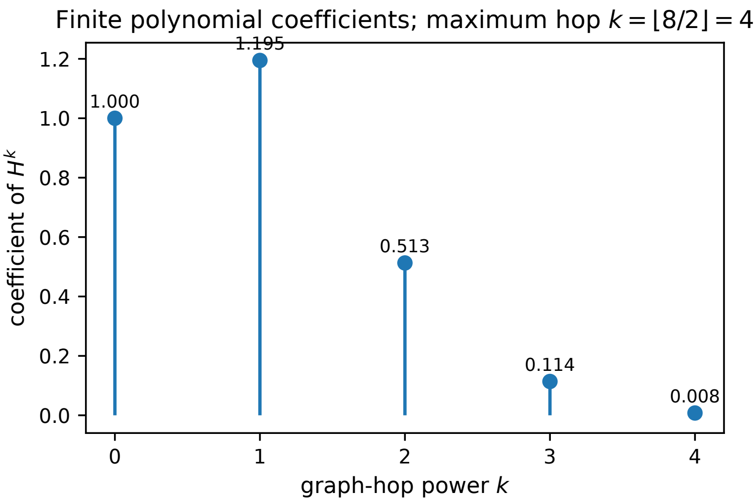

Figure 2. Coefficient profile of the finite graph polynomial in Eq 6.5. The largest graph-operator power is H^4, which agrees with the lacunary hop bound $\lfloor n/m \rfloor = \lfloor 8/2 \rfloor = 4$.

Applying the filter to the unit impulse $e_1 = (1, 0, 0, 0, 0)^T$ gives the response in Table 3 and Figure 3. The nonzero fifth component is consistent with the fact that vertex 5 is exactly four graph hops away from vertex 1; reducing the polynomial degree below four would force this component to vanish by Proposition 6.1.

Table 3. Response of the heterogeneous path-graph filter $\mathcal{F}^{(2,0)}_{8,0.6}(H; 0.20, 1)e_1$.

Vertex	Heterogeneous mass m_i	Filter response
1	1.00	3.26786868
2	2.00	−1.78624682
3	0.75	0.39872549
4	1.50	−0.07294505
5	1.25	0.00205581

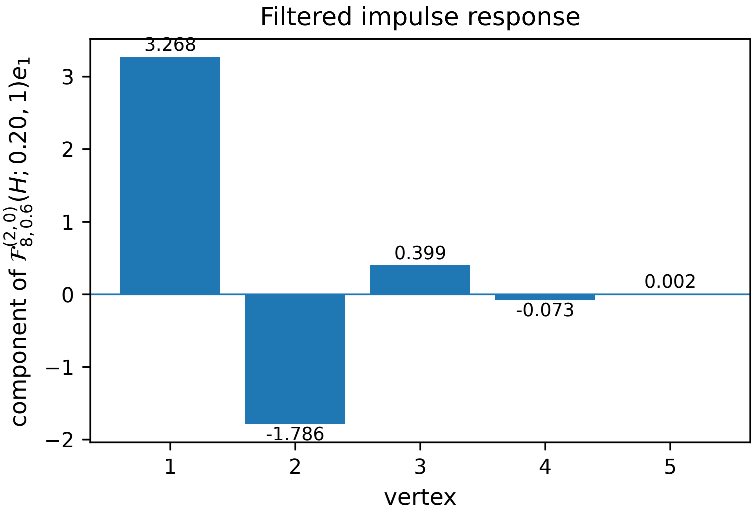

Figure 3. Filtered impulse response $\mathcal{F}^{(2,0)}_{8,0.6}(H; 0.20, 1)e_1$ on the heterogeneous path graph. The alternating signs reflect the off-diagonal structure of the mass-weighted Laplacian H.

The spectral viewpoint is shown in Figure 4. For the present graph,

$$\sigma(H) \approx \{0,\ 0.24246472,\ 1.08929226,\ 1.62667419,\ 3.61490216\},$$

and the plotted curve is the scalar polynomial corresponding to Eq 6.5. This confirms that the construction may be read either as a localized finite-hop vertex-domain filter or as a polynomial spectral multiplier on the eigenvalues of the heterogeneous graph operator.

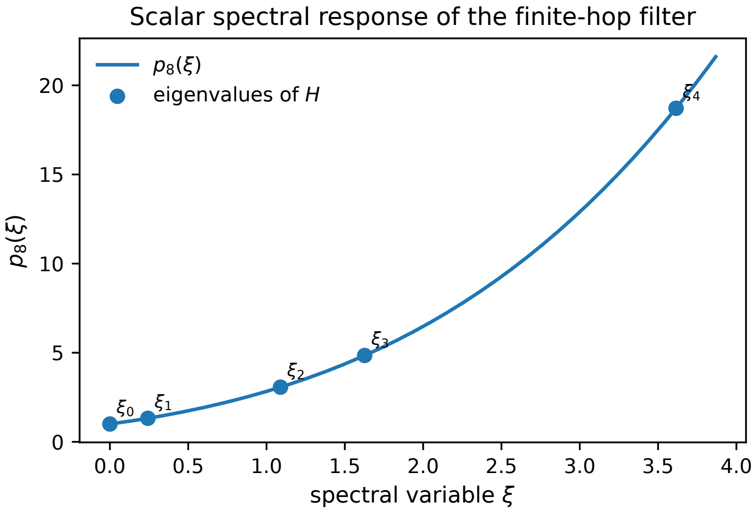

Figure 4. Scalar spectral response $p_8(\xi)$ of the finite-hop graph filter in Eq 6.5. Markers indicate the eigenvalues of the heterogeneous graph Laplacian $H = M^{-1/2} L_G M^{-1/2}$.

This graph-filter interpretation assigns a concrete role to the polynomial family in network and heterogeneous-media computations: the same finite coefficient formula that drives the symbolic theory produces a localized operator for heterogeneous diffusion data on a graph while preserving a transparent spectral response.

6.2. A 24-node graph and comparison with a Chebyshev filter

To test the same filter mechanism on a more complex graph, we next use a deterministic heterogeneous weighted graph with $N = 24$ vertices and 40 undirected weighted edges. The graph contains a weighted cycle together with longer-range weighted chords; the edge weights lie in the interval $[0.2500, 1.3449]$, while the nodal masses lie in $[0.5800, 1.4350]$. The associated mass-weighted Laplacian has spectral range

$$0 = \xi_1 < \xi_2 \approx 0.3913, \qquad \xi_{24} \approx 6.5239.$$

The graph is shown in Figure 5.

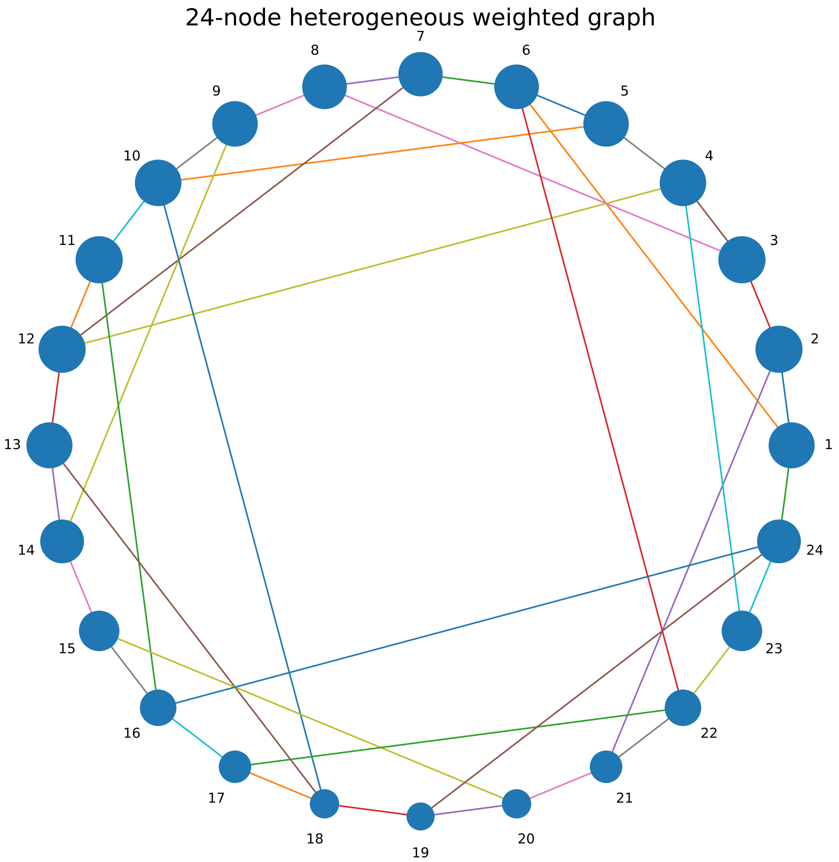

Figure 5. A 24-node heterogeneous weighted graph used for the larger graph-filter test. Node sizes are proportional to the masses, and the additional chords make the example non-path-like while preserving sparse local structure.

For this graph, we take

$$(m, \lambda, q, n, \tau, \eta) = (3, 1, 0.65, 11, 0.02, -1), \qquad A_q(t) \equiv 1.$$

Since $\lfloor n/m \rfloor = 3$, the normalized filter has hop radius three and scalar response

$$\widetilde{p}(\xi) = 1 - 0.27073770\xi + 0.03143747\xi^2 - 0.00158799\xi^3. \tag{6.6}$$

The response decreases on the computed spectral interval and therefore behaves as a low-pass multiplier for this parameter set. As a standard polynomial benchmark, we also compute a degree-three Chebyshev approximation to the heat multiplier $g(\xi) = e^{-0.30\xi}$ on $[0, 6.5239]$. In ordinary powers of ξ, this Chebyshev benchmark is approximately

$$\widetilde{p}_{\mathrm{Ch}}(\xi) = 0.996227 - 0.287606\xi + 0.035562\xi^2 - 0.001784\xi^3. \tag{6.7}$$

Figure 6 compares the two polynomial responses with the target heat curve, and Table 4 reports representative gains at selected eigenvalues. The Chebyshev polynomial is optimized for the heat target, whereas Eq 6.6 is not fitted to that target and is instead generated directly by the q-Laguerre–Sheffer structure. Thus the comparison is not a like-for-like heat-kernel optimization test; the similar behavior over the observed spectrum highlights the utility of the proposed construction as a generic low-pass multiplier with built-in finite-hop locality.

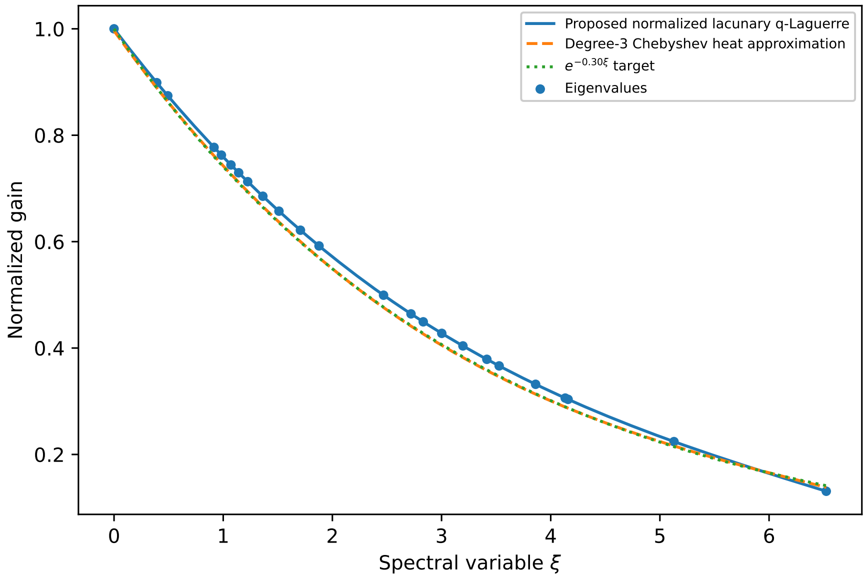

Figure 6. Spectral comparison on the 24-node heterogeneous graph. The proposed normalized lacunary q-Laguerre filter is plotted against a degree-three Chebyshev approximation of $e^{-0.30\xi}$; markers indicate eigenvalues of H.

Table 4. Selected spectral gains for the 24-node graph.

Eigenvalue index	ξ_i	Proposed gain $\widetilde{p}(\xi_i)$	Chebyshev gain $\widetilde{p}_{\mathrm{Ch}}(\xi_i)$
1	0.0000	1.0000	0.9962
6	1.0710	0.7442	0.7268
11	1.7074	0.6215	0.6000
16	3.0020	0.4276	0.4051
21	4.1329	0.3059	0.2891
24	6.5239	0.1308	0.1382

The vertex-domain locality is also visible. Applying Eq 6.6 to a unit impulse at vertex 1 produces Figure 7. The only vertices at distance four from vertex 1 are vertices 9, 13, and 14, and the corresponding entries are zero up to machine precision, exactly as predicted by Proposition 6.1.

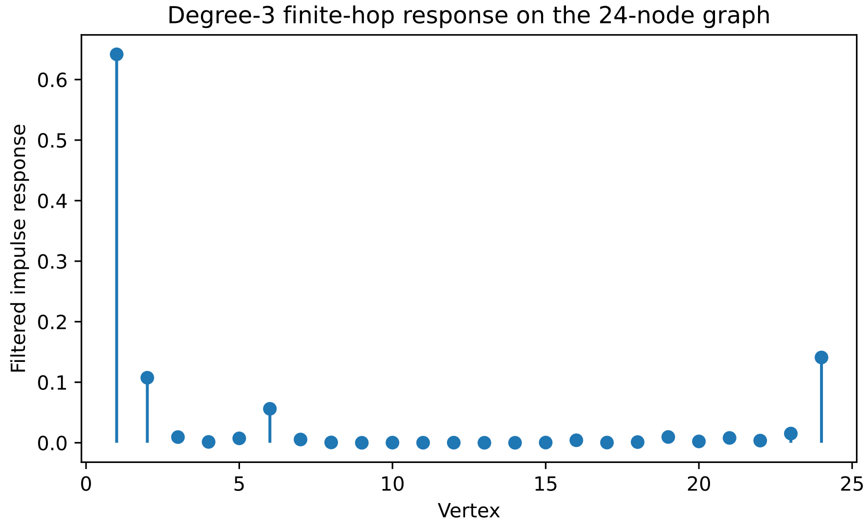

Figure 7. Impulse response of the degree-three normalized filter in Eq 6.6 on the 24-node graph. Vertices outside three hops from the source have zero response.

Finally, the same graph allows a simple non-exponential Sheffer test. Choosing the invertible quadratic factor

$$A_{q,\beta}(t) = 1 + \beta \frac{t^2}{[\,2\,]_q!}, \qquad \beta = -0.05,$$

gives a genuine Sheffer deformation that is not a q-translation. Because β enters only through $A_{q,\beta}$, the quadratic factor supplies an additional tuning parameter independent of τ, η, and q. After normalizing to unit gain at $\xi = 0$, the resulting degree-three response is

$$1 - 0.275794\xi + 0.034020\xi^2 - 0.001990\xi^3,$$

so the high-frequency gain at ξ_{24} changes from 0.1308 in the core case to 0.0961. This confirms that the general Sheffer factor can be used numerically to tune the spectral multiplier, not only as a formal algebraic device.

6.3. *Example I: the core family $A_q(t) \equiv 1$*

We fix $(m, \lambda, q) = (2, 0, 0.6)$ and $x_0 = 0.7$. Figure 8 displays the profiles $y \mapsto \mathcal{L}_{n,q}^{(2,0)}(x_0, y)$ for several values of n, while Figure 9 shows the complex zeros of the polynomial $\mathcal{L}_{8,q}^{(2,0)}(x_0, y)$ with respect to y.

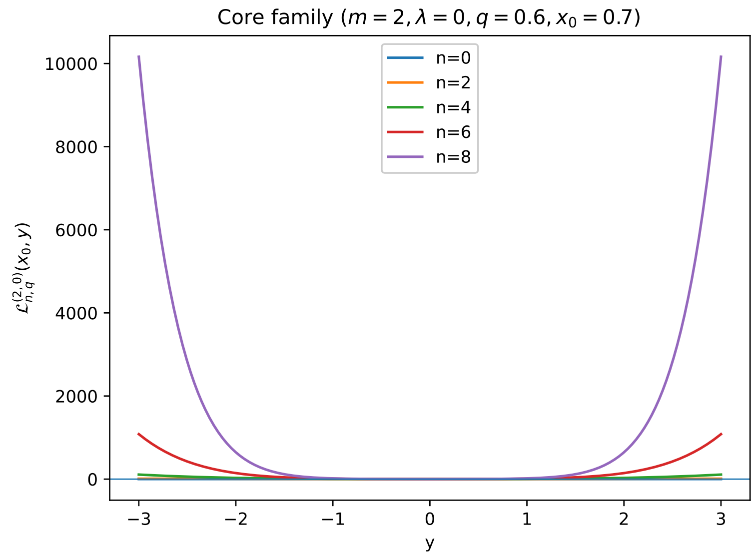

Figure 8. Profiles of the core polynomials $\mathcal{L}^{(2,0)}_{n,q}(x_0, y)$ for $n \in \{0, 2, 4, 6, 8\}$ with $(q, x_0) = (0.6, 0.7)$.

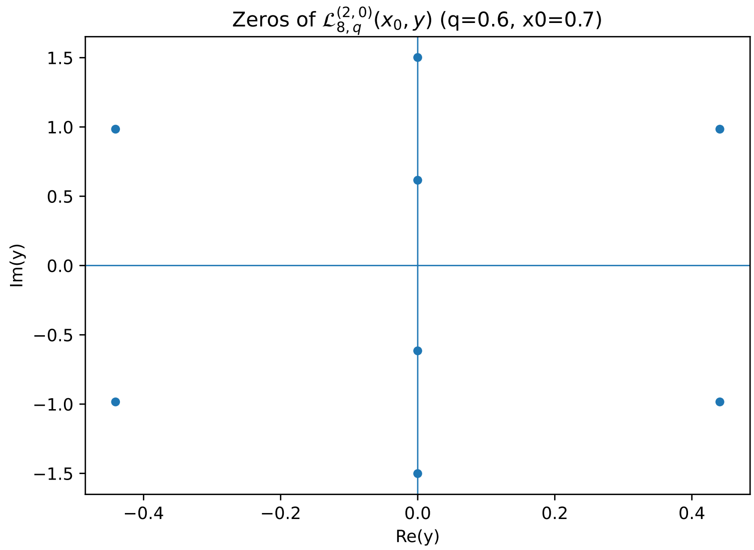

Figure 9. Zeros of $\mathcal{L}^{(2,0)}_{8,q}(x_0, y)$ in the complex y-plane for $(q, x_0) = (0.6, 0.7)$.

For this example, the coefficient formula gives

$$\mathcal{L}^{(2,0)}_{8,q}(0.7, y) = y^8 + 4.1811018593y^6 + 6.2823544028y^4 + 4.8822868502y^2 + 1.1548445593.$$

Thus, the polynomial is even in y, as predicted by the residue-class profile in Proposition 3.6. Its eight zeros consist of four conjugate pairs, no real zeros occur, and the moduli lie between 0.6155703435 and 1.5013570155. The values at $y = 1$ for $n = 0, 2, 4, 6, 8$ are 1.0000000000, 2.1200000000, 5.2916160000, 10.6402295527, and 17.5005876716. Table 5 summarizes the corresponding degree and zero diagnostics, respectively.

Table 5. Numerical diagnostics for the core case $(m, \lambda, q, x_0) = (2, 0, 0.6, 0.7)$.

Quantity	Value	Interpretation	Source formula
$\deg_y \mathcal{L}_{8,q}^{(2,0)}$	8	leading y-degree	Eq 3.5
$\deg_x \mathcal{L}_{8,q}^{(2,0)}$	4	lacunary depth $\lfloor 8/2 \rfloor$	Eq 3.6
Number of real zeros in y	0	zeros are non-real conjugate pairs	direct root computation
Minimum zero modulus	0.6155703435	inner zero radius	direct root computation
Maximum zero modulus	1.5013570155	outer zero radius	direct root computation

6.4. A kernel truncation diagnostic

To quantify numerical truncation effects for the q-Tricomi-Bessel kernel in Eq 2.9, we consider the partial sums

$$C_{\lambda,q}^{(K)}(x) = \sum_{k=0}^{K} \frac{(-1)^k x^k}{[\,k\,]_q!\,[\,\lambda + k\,]_q!} \qquad (K \in \mathbb{N}_0),$$

and monitor the absolute truncation error $|C_{\lambda,q}(x) - C_{\lambda,q}^{(K)}(x)|$. Figure 10 shows this error for $(\lambda, q, x) = (1, 0.6, 0.9)$.

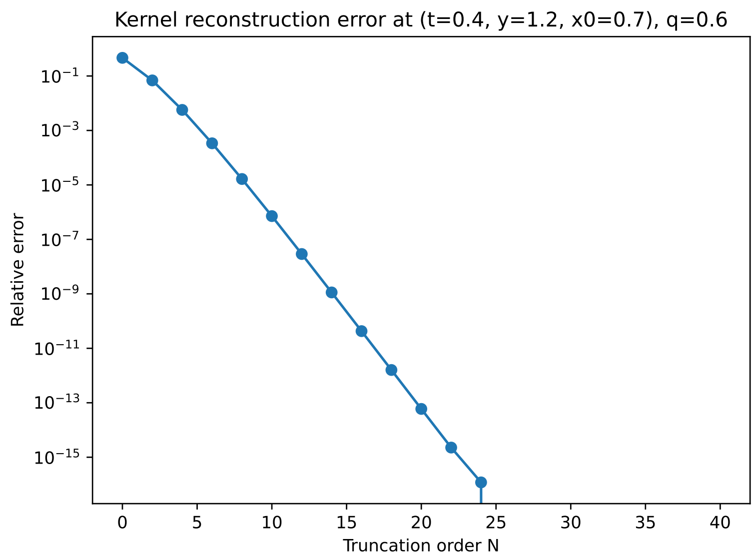

Figure 10. Truncation error for $C_{1,q}(x)$ at $x = 0.9$ with $q = 0.6$, as a function of the truncation order K.

Table 6 gives representative absolute errors. The rapid decrease confirms that, for the parameter range used in the illustrations, a modest truncation order already gives stable numerical values of the kernel. This check is useful because all finite polynomial evaluations in Eq 3.3 use the same q-factorial scale as the kernel series. The parameter q also affects the tail behavior of the kernel series. Indeed, the ratio of consecutive absolute kernel terms is

$$\frac{|x|}{[\,k+1\,]_q\,[\,\lambda + k + 1\,]_q},$$

which tends to $|x|(1-q)^2$ as $k \to \infty$. Hence, within the convergence regime, smaller values of q generally enlarge the asymptotic ratio and can slow the decay of the tail, whereas values of q closer to 1 reduce the tail ratio and usually improve truncation stability. The same dependence should be kept in mind when evaluating the finite polynomial sums, because slowly decaying kernel coefficients can amplify round-off sensitivity in higher-degree computations.

Table 6. Absolute truncation error $|C_{1,0.6}(0.9) - C^{(K)}_{1,0.6}(0.9)|$.

K	4	8	12	16
Error	8.6576×10^{-4}	4.4300×10^{-7}	1.9476×10^{-10}	8.4044×10^{-14}

6.5. *Example II: a Sheffer twist $A_q(t) = e_q(\alpha t)$*

A convenient and widely used deformation is obtained by choosing

$$A_q(t) = e_q(\alpha t) = \sum_{j\geq 0} \alpha^j \frac{t^j}{[\,j\,]_q!},$$

so that $a_j = \alpha^j$ in Eq 3.1. We fix $(m, \lambda, q) = (3, 1, 0.6)$ and $x_1 = 0.5$. Figure 11 compares the core case $A_q(t) \equiv 1$ against the twist with $\alpha = 0.8$ for $n = 9$, and Figure 12 illustrates the sensitivity of the scalar response $\alpha \mapsto \mathcal{L}^{(3,1;\alpha)}_{9,q}(x_1, 1)$.

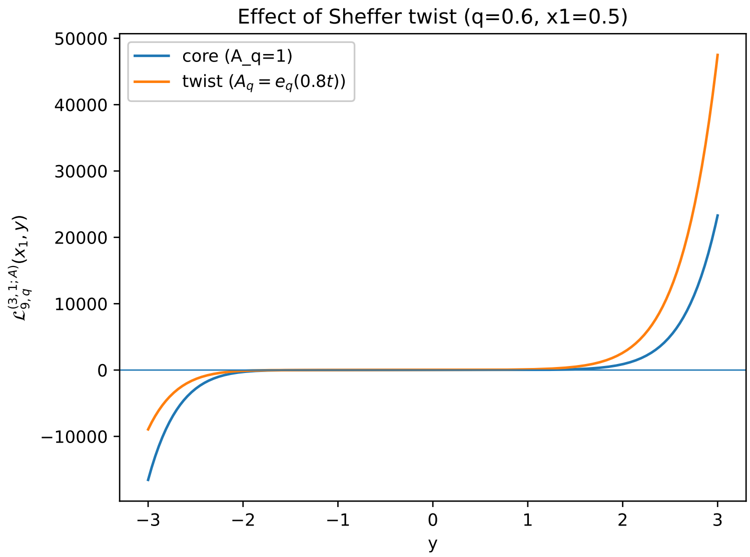

Figure 11. Core vs. Sheffer-twisted profiles of $\mathcal{L}^{(3,1;A)}_{9,q}(x_1, y)$ for $(q, x_1) = (0.6, 0.5)$ and $\alpha = 0.8$.

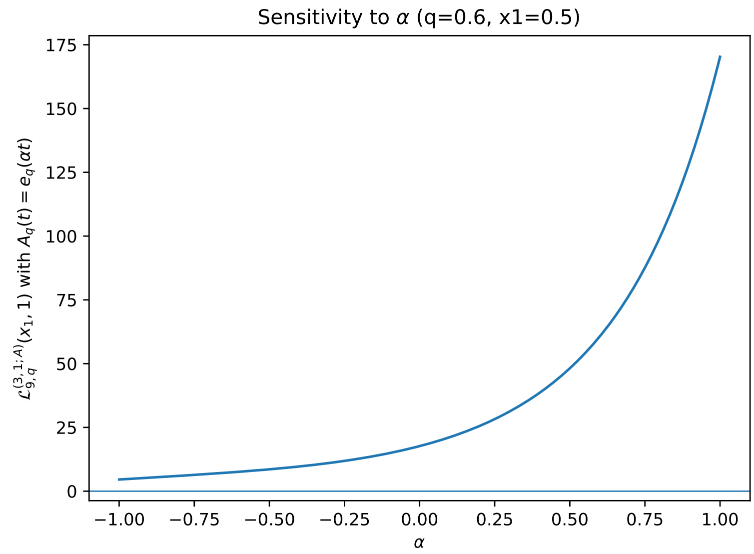

Figure 12. Sensitivity of $\mathcal{L}_{9,q}^{(3,1;\alpha)}(x_1, 1)$ with respect to $\alpha \in [-1, 1]$ for $(q, x_1) = (0.6, 0.5)$.

The scalar response in Figure 12 is the ninth-degree polynomial

$$\begin{aligned}\mathcal{L}_{9,q}^{(3,1;\alpha)}(0.5, 1) = 17.6637585086 &+ 30.7454718805\alpha + 36.9278567575\alpha^2 \\ &+ 31.1335781408\alpha^3 + 21.0277433105\alpha^4 + 16.1724878712\alpha^5 \\ &+ 9.3330364567\alpha^6 + 3.8019351976\alpha^7 + 2.4748057600\alpha^8 + \alpha^9.\end{aligned}$$

On the interval $[-1, 1]$ its derivative is positive in the sampled computation; in particular,

$$\frac{d}{d\alpha}\mathcal{L}_{9,q}^{(3,1;\alpha)}(0.5, 1)\bigg|_{\alpha=0.8} \approx 256.7806485224.$$

This provides numerical evidence for the identifiability of α in the calibration experiment below.

6.6. *A one-parameter calibration problem in α*

Assume that (m, λ, q) and (x_1, y_1) are prescribed and that the Sheffer deformation is of exponential type, $A_q(t) = e_q(\alpha t)$, but the parameter α is unknown. For a fixed index n, we may use the scalar observation

$$T = \mathcal{L}_{n,q}^{(m,\lambda;\alpha)}(x_1, y_1)$$

to recover α. Since Eq 3.3 is finite in j, the mapping $\alpha \mapsto \mathcal{L}_{n,q}^{(m,\lambda;\alpha)}(x_1, y_1)$ is a polynomial in α of degree at most n:

$$\mathcal{L}_{n,q}^{(m,\lambda;\alpha)}(x_1, y_1) = \sum_{j=0}^{n} c_j \alpha^j, \qquad c_j = \frac{[n]_q!}{[j]_q!} \sum_{k=0}^{\lfloor (n-j)/m \rfloor} \frac{x_1^k y_1^{n-mk-j}}{[n-mk-j]_q!\,[k]_q!\,[\lambda+k]_q!}. \tag{6.8}$$

Thus, the calibration equation $\mathcal{L}_{n,q}^{(m,\lambda;\alpha)}(x_1, y_1) = T$ reduces to a univariate polynomial root problem.

For an explicit numerical illustration, we take the parameters of Example II with $(n, y_1) = (9, 1)$ and generate a synthetic target from $\alpha^\star = 0.8$, namely

$$T = \mathcal{L}_{9,q}^{(3,1;\alpha^\star)}(x_1, 1) \approx 99.5400651768.$$

Figure 13 plots the least-squares objective $J(\alpha) = (\mathcal{L}_{9,q}^{(3,1;\alpha)}(x_1, 1) - T)^2$, and Figure 14 plots the residual $R(\alpha) = \mathcal{L}_{9,q}^{(3,1;\alpha)}(x_1, 1) - T$. Solving the polynomial equation obtained from Eq 6.8 yields the real solution

$$\widehat{\alpha} = 0.800,$$

which coincides with the prescribed value $\alpha^\star$ up to numerical precision. For this particular coefficient set, a numerical real-root computation gives one real root and four non-real conjugate pairs. In addition, the sampled derivative of the residual is positive on $[-1, 1]$, so uniqueness on the calibration interval is supported numerically. We do not claim a general uniqueness theorem for arbitrary $(m, \lambda, q, n, x_1, y_1, T)$; the statement is empirical for the present parameter set.

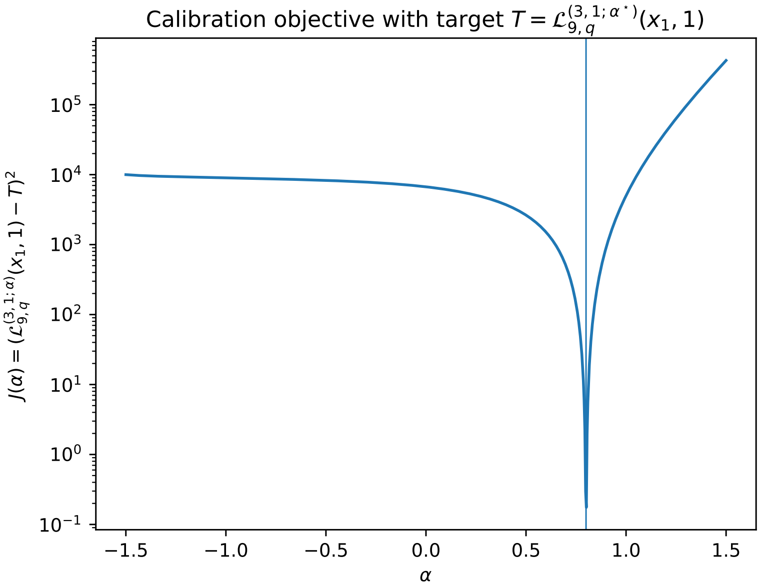

Figure 13. Calibration objective $J(\alpha)$ for recovering α from the target T. The vertical line indicates $\alpha^\star = 0.8$.

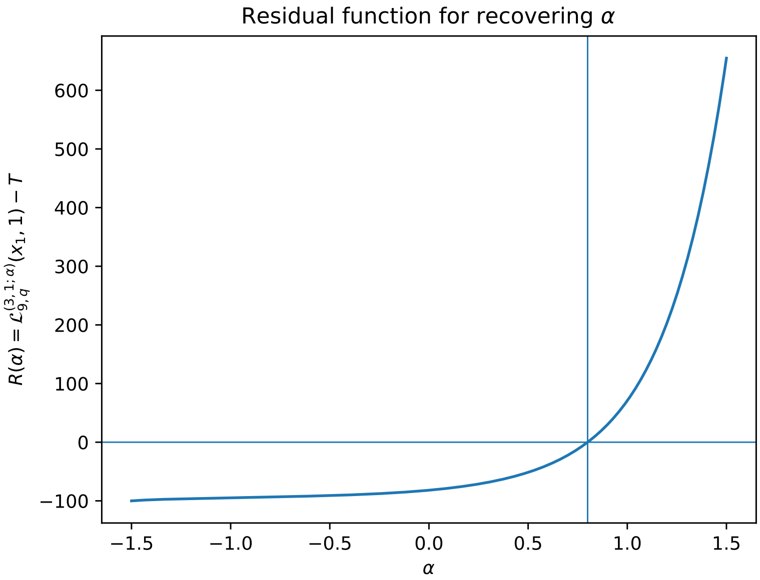

Figure 14. Residual function $R(\alpha) = \mathcal{L}^{(3,1;\alpha)}_{9,q}(x_1, 1) - T$ for the calibration problem.

7. Conclusions

We constructed a Sheffer-type (m, λ)-lacunary bivariate q-Laguerre family generated by

$$A_q(t)\, e_q(yt)\, C_{\lambda,q}(-xt^m),$$

where m induces residue-class lacunarity, λ controls the order of the q-Tricomi-Bessel kernel, and $A_q(t)$ provides a general invertible Sheffer deformation. The simultaneous presence of these three ingredients is the main structural novelty of the paper: earlier bivariate q-Laguerre, q-Laguerre-Appell, and lacunary Laguerre constructions are recovered by suppressing one or more of them, whereas the present model keeps all three and therefore links the corresponding coefficient, lowering, and translation mechanisms in a single framework.

The main results are: (i) an explicit finite coefficient formula and residue-class profile; (ii) a q-binomial Sheffer convolution law; (iii) compatible y- and x-lowering relations, including the kernel-order shift; (iv) an operational representation with quasi-monomial raising and lowering operators; (v) the induced operator q-difference equation and q-translation identity; and (vi) the classical limit $q \to 1^-$. The graph-filter section shows that evaluating the polynomials at τH and ηI gives a finite-hop spectral multiplier for the heterogeneous operator $H = M^{-1/2} L_G M^{-1/2}$, with hop radius bounded by $\lfloor n/m \rfloor$.

The numerical part includes both a small path graph, which makes the locality mechanism transparent, and a 24-node heterogeneous graph, which gives a more realistic sparse-network test. The larger example compares the proposed polynomial response with a degree-three Chebyshev heat-filter approximation and also demonstrates a non-exponential quadratic Sheffer factor. These computations indicate that m, λ, τ, η, and A_q can be used to tune locality and spectral shape while preserving an explicit finite-sum representation.

The graph-theoretic contribution should be distinguished from recent exact spectral studies, such as Banerjee and Ganguly's work on Laplacian and distance Laplacian spectra of generalized fan graphs and a new graph class [39], and Banerjee's work on signless Laplacian spectra of power graphs of finite non-commutative groups [40, 41]. Those papers determine spectra and related structural data for specified graph classes. In contrast, the present paper uses the mass-weighted Laplacian of a heterogeneous weighted graph as the argument of a lacunary q-Laguerre-Sheffer polynomial. Thus, the common ground is the Laplacian/spectral graph-theory setting, while the new aspect here is a tunable finite-hop graph filter whose support radius is controlled by $\lfloor n/m \rfloor$ and whose spectral response is shaped by λ, q, τ, η, and A_q.

The present study also has limitations. The graph experiments remain illustrative rather than large-scale benchmark tests, and the non-exponential Sheffer example uses a single quadratic deformation. The calibration experiment establishes recoverability only for a synthetic one-parameter case and supplies numerical evidence of uniqueness for that parameter set, not a global identifiability theorem. In addition, no orthogonality, positivity, or stability theory is proved for arbitrary Sheffer factors.

Several future directions are natural. One may develop stable recurrence-based algorithms for high-degree evaluation and compare them systematically with direct coefficient summation; study positivity, zero localization, and possible orthogonality regimes under additional restrictions on A_q, m, and λ; extend the graph-filter construction to adaptive or learned Sheffer factors on large heterogeneous networks; and formulate inverse problems in which a finite set of graph or scalar observations is used to recover multiple coefficients of $A_q(t)$ rather than a single exponential-twist parameter. Further work may also consider fractional or variable-order q-difference analogues and multivariate lacunary kernels for higher-dimensional networked or tensor-product models.

Use of AI tools declaration

The authors declare they have not used Artificial Intelligence (AI) tools in the creation of this article.

Acknowledgments

The researchers would like to thank the Deanship of Graduate Studies and Scientific Research at Qassim University (https://www.qu.edu.sa) for the financial support provided for the publication of this research under the APC funding program (Grant No. QU-APC-2026).

Conflict of interest

The authors declare there is no conflict of interest.

Author contributions

Waseem Ahmad Khan: Conceptualization, Methodology, Formal analysis, Validation, Writing–review & editing.

Oğuz Yağcı: Conceptualization, Methodology, Formal analysis, Investigation, Writing–original draft.

Khidir Shaib Mohamed: Conceptualization, Supervision, Project administration, Funding acquisition, Validation, Writing–review & editing.

Azhar Iqbal: Investigation, Formal analysis, Visualization, Writing–review & editing.

Wei Sin Koh: Investigation, Validation, Visualization, Writing–review & editing.
Naglaa Mohammed: Investigation, Formal analysis, Visualization, Writing–review & editing.
All authors have read and approved the final version of the manuscript.

Data availability statement

No external datasets were used in this study.

References

1. F. H. Jackson, q-difference equations, *Amer. J. Math.*, **32** (1910), 305–314. https://doi.org/10.2307/2370183
2. V. Kac, P. Cheung, *Quantum Calculus*, Springer, New York, 2002. https://doi.org/10.1007/978-1-4613-0071-7
3. G. Gasper, M. Rahman, Basic hypergeometric series, in *Encyclopedia of Mathematics and its Applications*, 2nd ed., Cambridge University Press, Cambridge, (2004), 1–37. https://doi.org/10.1017/CBO9780511526251
4. R. Koekoek, P. A. Lesky, R. F. Swarttouw, *Hypergeometric Orthogonal Polynomials and Their q-Analogues*, Springer Monographs in Mathematics, Springer, Berlin, 2010. https://doi.org/10.1007/978-3-642-05014-5
5. D. S. Moak, The q-analogue of the Laguerre polynomials, *J. Math. Anal. Appl.*, **81** (1981), 20–47. https://doi.org/10.1016/0022-247X(81)90048-2
6. R. Askey, Limits of some q-Laguerre polynomials, *J. Approx. Theory*, **46** (1986), 213–216. https://doi.org/10.1016/0021-9045(86)90062-6
7. J. Cigler, Operator methods for q-identities. II. q-Laguerre polynomials, *Monatsh. Math.*, **91** (1981), 105–117. https://doi.org/10.1007/BF01295141
8. J. Cao, N. Raza, M. Fadel, Two-variable q-Laguerre polynomials from the context of quasi-monomiality, *J. Math. Anal. Appl.*, **535** (2024), 128126. https://doi.org/10.1016/j.jmaa.2024.128126
9. Q. Bao, D. Yang, Notes on q-partial differential equations for q-Laguerre polynomials and little q-Jacobi polynomials, *Fundam. J. Math. Appl.*, **7** (2024), 59–76. https://doi.org/10.33401/fujma.1365120
10. N. Ahmad, W. A. Khan, A new generalization of q-Laguerre-based Appell polynomials and quasi-monomiality, *Symmetry*, **17** (2025), 439. https://doi.org/10.3390/sym17030439
11. H. Qawaqneh, W. A. Khan, H. Aydi, U. Duran, C. S. Ryoo, A comprehensive study of generalized bivariate q-Laguerre polynomials: Structural properties and applications, *Eur. J. Pure Appl. Math.*, **18** (2025), 6668. https://doi.org/10.29020/nybg.ejpam.v18i3.6668
12. M. Zayed, W. A. Khan, C. S. Ryoo, U. Duran, An exploratory study on bivariate extended q-Laguerre-based Appell polynomials with some applications, *AIMS Math.*, **10** (2025), 12841–12867. https://doi.org/10.3934/math.2025577

13. M. Kumar, N. Raza, W. Ramírez, On the theory and applications of q-Mittag-Leffler-Laguerre polynomials, *Dolomites Res. Notes Approx.*, **18** (2025), 118–134. https://doi.org/10.25430/pupj-DRNA-2025-1-10
14. P. Appell, On a class of polynomials, *Ann. Sci. Éc. Norm. Supér.*, **9** (1880), 119–144. https://doi.org/10.24033/asens.186
15. I. M. Sheffer, Some properties of polynomial sets of type zero, *Duke Math. J.*, **5** (1939), 590–622. https://doi.org/10.1215/S0012-7094-39-00549-1
16. G. C. Rota, D. Kahaner, A. Odlyzko, On the foundations of combinatorial theory. VIII. Finite operator calculus, *J. Math. Anal. Appl.*, **42** (1973), 684–760. https://doi.org/10.1016/0022-247X(73)90172-8
17. S. Roman, The umbral calculus, in *Pure and Applied Mathematics*, Academic Press, New York, **111** (1984). Available from: https://search.worldcat.org/title/11866043.
18. S. Khan, N. Raza, Monomiality principle, operational methods and family of Laguerre–Sheffer polynomials, *J. Math. Anal. Appl.*, **387** (2012), 90–102. https://doi.org/10.1016/j.jmaa.2011.08.064
19. Z. Özat, B. Çekim, M. A. Özarslan, Laguerre-type general-Appell polynomials, *Integr. Transforms Spec. Funct.*, **36** (2025), 571–589. https://doi.org/10.1080/10652469.2024.2418889
20. W. A. Khan, K. S. Mohamed, F. A. Costabile, S. A. Wani, A. Adam, A new generalization of mth-order Laguerre-based Appell polynomials associated with two-variable general polynomials, *Mathematics*, **13** (2025), 2179. https://doi.org/10.3390/math13132179
21. M. Fadel, W. Ramírez, C. Cesarano, S. Díaz, q-Legendre based Gould–Hopper polynomials and q-operational methods, *Ann. Univ. Ferrara*, **71** (2025), 32. https://doi.org/10.1007/s11565-025-00587-z
22. G. Dattoli, M. Migliorati, H. M. Srivastava, Some families of generating functions for the Bessel and related functions, *Georgian Math. J.*, **11** (2004), 219–228. https://doi.org/10.1515/GMJ.2004.219
23. M. Riyasat, T. Nahid, S. Khan, q-Tricomi functions and quantum algebra representations, *Georgian Math. J.*, **28** (2021), 793–803. https://doi.org/10.1515/gmj-2020-2079
24. T. Nahid, H. P. Rani, Mittag-Leffler based Bessel and Tricomi functions via umbral approach, *Rep. Math. Phys.*, **92** (2023), 1–17. https://doi.org/10.1016/S0034-4877(23)00051-4
25. M. Fadel, N. Raza, W. S. Du, Characterizing q-Bessel functions of the first kind with their new summation and integral representations, *Mathematics*, **11** (2023), 3831. https://doi.org/10.3390/math11183831
26. U. Zainab, M. Kumar, N. Raza, Borel transform and integral identities involving λ-Bessel and λ-Tricomi matrix functions, *Math. Methods Appl. Sci.*, **48** (2025), 3253–3271. https://doi.org/10.1002/mma.10483
27. D. Babusci, G. Dattoli, K. Górska, K. A. Penson, Lacunary generating functions for the Laguerre polynomials, *Séminaire Lotharingien de Combinatoire*, **76** (2017), B76b. Available from: https://arxiv.org/abs/1302.4894.
28. F. R. K. Chung, Spectral graph theory, in *CBMS Regional Conference Series in Mathematics*, American Mathematical Society, Providence, RI, **92** (1997). Available from: https://bookstore.ams.org/cbms-92.

29. D. I. Shuman, S. K. Narang, P. Frossard, A. Ortega, P. Vandergheynst, The emerging field of signal processing on graphs: Extending high-dimensional data analysis to networks and other irregular domains, *IEEE Signal Process. Mag.*, **30** (2013), 83–98. https://doi.org/10.1109/MSP.2012.2235192
30. D. Mugnolo, *Semigroup Methods for Evolution Equations on Networks*, Understanding Complex Systems, Springer, Cham, 2014. https://doi.org/10.1007/978-3-319-04621-1
31. T. Liu, R. Xue, A convergent multi-step efficient iteration method to solve nonlinear equation systems, *J. Appl. Math. Comput.*, **71** (2025), 2571–2588. https://doi.org/10.1007/s12190-024-02324-9
32. T. Liu, B. Ding, A radial basis function neural network approach for solving a diffusion partial differential equation efficiently, *Appl. Math. Comput.*, **509** (2026), 129651. https://doi.org/10.1016/j.amc.2025.129651
33. T. Liu, R. Xue, M. Barfeie, A unified framework for high-order compact finite differences using infinitely- and piecewise-smooth RBFs with polynomials, *Calcolo*, **63** (2026), 18. https://doi.org/10.1007/s10092-026-00684-1
34. Y. Liu, Y. Li, T. Liu, An RBF–FD method for pricing under the Bates model: Handling stochastic volatility and jump processes, *Eng. Anal. Bound. Elem.*, **183** (2026), 106622. https://doi.org/10.1016/j.enganabound.2025.106622
35. Y. Liu, Y. Ding, F. Soleymani, Polynomial approximation and tensor-product iterative methods for Rayleigh–Tail and fractional Rayleigh–Tail integral equations, *Comput. Appl. Math.*, **45** (2026), 173. https://doi.org/10.1007/s40314-025-03477-4
36. F. W. J. Olver, A. B. Olde Daalhuis, D. W. Lozier, B. I. Schneider, R. F. Boisvert, C. W. Clark, et al., *NIST Digital Library of Mathematical Functions*, Release 1.2.7, 2026. Available from: https://dlmf.nist.gov/10.2.
37. D. K. Hammond, P. Vandergheynst, R. Gribonval, Wavelets on graphs via spectral graph theory, *Appl. Comput. Harmon. Anal.*, **30** (2011), 129–150. https://doi.org/10.1016/j.acha.2010.04.005
38. M. Defferrard, X. Bresson, P. Vandergheynst, Convolutional neural networks on graphs with fast localized spectral filtering, *Adv. Neural Inf. Process. Syst.*, **29** (2016). Available from: https://arxiv.org/abs/1606.09375.
39. S. Banerjee, S. Ganguly, On Laplacian and distance Laplacian spectra of generalized fan graph and a new graph class, *Int. J. Math. Comput. Eng.*, **3** (2025), 293–306. https://doi.org/10.2478/ijmce-2025-0021
40. S. Banerjee, Signless Laplacian spectrum of power graph of certain finite non-commutative groups, *Int. J. Math. Comput. Eng.*, **4** (2026), 33–44. https://doi.org/10.2478/ijmce-2026-0003
41. A. Kiran, M. Yaseen, A. Khan, T. Abdeljawad, M. A. Alqudah, R. Thinakaran, Solving time fractional diffusion-wave equation using hyperbolic polynomial B-splines: A uniform grid approach, *Ain Shams Eng. J.*, **17** (2026), 103868. https://doi.org/10.1016/j.asej.2025.103868